
Article:
Zheng, F., Zhu, D., Giles, M. et al. (4 more authors) (2019) Mineral and organic fertilization alters the microbiome of a soil nematode Dorylaimus stagnalis and its resistome. The Science of The Total Environment, 680. pp. 70-78. ISSN 0048-9697

https://doi.org/10.1016/j.scitotenv.2019.04.384

Mineral and organic fertilization alters the microbiome of a soil nematode *Dorylaimus stagnalis* and its resistome

Fei Zheng[a,b,#], Dong Zhu [a,b,#], Madeline Giles[c], Tim Daniell[c,d], Roy Neilson[c], Yong-Guan Zhu[a,b,e], Xiao-Ru Yang[a,*]

[a] *Key Laboratory of Urban Environment and Health, Institute of Urban Environment, Chinese Academy of Sciences, 1799 Jimei Road, Xiamen 361021, China.*

[b] *University of the Chinese Academy of Sciences, 19A Yuquan Road, Beijing 100049, China.*

[c] *Ecological Sciences, The James Hutton Institute, Dundee, DD2 5DA, Scotland, UK.*

[d] *Department of Animal and Plant Sciences, The University of Sheffield, Sheffield, S10 2TN, UK.*

[e] *State Key Laboratory of Urban and Regional Ecology, Research Center for Eco-Environmental Sciences, Chinese Academy of Sciences, Beijing 100085, China.*

[#] Fei Zheng and Dong Zhu contributed equally to this paper.

* Corresponding author: Xiao-Ru Yang

Key Laboratory of Urban Environment and Health, Institute of Urban Environment, Chinese Academy of Sciences, No.1799 Jimei Road, Xiamen 361021, China.

* E-mail address: xryang@iue.ac.cn. Tel: +86 592- 6190560; Fax: +86 592-6190977.

ABSTRACT

Although the effects of fertilization on the abundance and diversity of soil nematodes have been widely studied, the impact of fertilization on soil nematode microbiomes remains largely unknown. Here, we investigated how different fertilizers: no fertilizer, mineral fertilizer, clean slurry (pig manure with a reduced antibiotic burden) and dirty slurry (pig manure with antibiotics) affect the microbiome of a dominant soil nematode and its associated antibiotic resistance genes (ARGs). The results of 16S rRNA gene high throughput sequencing showed that the microbiome of the soil nematode *Dorylaimus stagnalis* is diverse (Shannon index: 9.95) and dominated by Proteobacteria (40.3%). Application of mineral fertilizers significantly reduced the diversity of the nematode microbiome (by 28.2%; $P < 0.05$) but increased the abundance of Proteobacteria (by 70.1%; $P = 0.001$). Microbial community analysis, using a null hypothesis model, indicated that microbiotas associated with the nematode are not neutrally assembled. Organic fertilizers also altered the diversity of the nematode microbiome, but had no impact on its composition as illustrated by principal coordinates analysis (PCoA). Interestingly, although no change of total ARGs was observed in the nematode microbiome and no significant relationship between nematode microbiome and resistome, the abundance of 48 out of a total of 75 ARGs was enriched in the organic fertilizer treatments. Thus, the data suggested that the ARGs in nematode microbiome still had a risk of horizontal gene transfer under fertilization and nematodes might be a potential refuge for ARGs.

Keywords: Mineral fertilizer, Pig manure, Microbial community, Antibiotic Resistance Genes, Refuge

1. Introduction

Soil nematodes are globally one of the most abundant and diverse invertebrate taxa (Yeates and Bongers, 1999; Wu et al., 2011; Ferris and Tuomisto, 2015; Zhang et al., 2015). They are an important component of the soil food web and participate in major soil processes (e.g. decomposition of organic matter, nutrient turnover, maintenance of biodiversity and energy transfer) (Ekschmitt et al., 2001; Rizvi and Mehta, 2009; Carrascosa et al., 2014; Sauvadet et al., 2016; Sechi et al., 2018). Nematodes are also commonly used as indicators of function and biodiversity of soil ecosystems (Yeates, 2003).

The nematode gut microbiome plays an important role in the nematodes performance, health and disease resistance as reported for bees, flies and nematodes (Gross, 2006; Engel and Moran, 2013; Berg et al., 2016; Stagaman et al., 2017). Recently, studies have characterized the microbiome of the model nematode species, *Caenorhabditis elegans* by using high-throughput sequencing (Berg et al., 2016; Clark and Hodgkin, 2016; Shapira, 2017; Zhang et al., 2017), whilst endosymbiont diversity has also been explored in a range of soil nematode taxa through various molecular approaches (Haegeman et al., 2009; Lazarova et al., 2016). In addition, the microbiome of *Haemonchus contortus*, an intestinal parasitic nematode of sheep (Sinnathamby et al., 2018), and the microbiomes found in a soil nematode from a grassland (Ladygina et al., 2009) have been identified using clone libraries, which indicated that a diverse microbial community inhabits nematodes. However, the exact community composition

of soil nematode microbiomes are poorly described due to technological difficulties, e.g. some rare bacteria groups are hard to detect using clone libraries (Agamennone et al., 2015). High-throughput sequencing has proven to be a powerful tool to characterize microbial communities at a higher resolution (Kautz et al., 2013; Zhu et al., 2018a; Zhu et al., 2018b). However, studies involving high-throughput sequencing mostly focus on *C. elegans*, which are usually sourced from controlled cultures (Felix et al., 2013).

With the increase in food demand, more fertilizers are being applied to soil ecosystems to supply nutrients for plants (Cui et al., 2013; Paerl et al., 2014; Boyle, 2017). Many studies have showed that fertilization can alter the abundance, diversity and function of soil nematodes (Biederman et al., 2008; Griffiths et al., 2010; Li et al., 2018). For example, application of mineral fertilizers could both significantly affect the community composition of soil nematodes and reduce their total abundance (Li et al., 2010). Meanwhile, the long-term application of organic manure can significantly increase total nematode abundance and diversity (Griffiths et al., 2010; Li et al., 2018), and short-term organic amendment application has a greater impact on the metabolic footprint (i.e. function) of nematodes than their abundance (Pan et al., 2017). However, the effects of fertilization on nematode microbiomes remain unknown. A change in the soil nematode microbiome may affect host health (Berg et al., 2016; Zhang et al., 2017), as the microbial community associated with the host can play an important role in nutrient absorption (Agamennone et al., 2015).

In China, pig manure is commonly applied to agricultural soil as a fertilizer as it has a high nutrient content and is produced in large quantities making it easily available (Boitt et al., 2018). However, additives in pig feed often contain antibiotics to promote growth and control disease, thus pig manure typically contains both antibiotics and bacterial communities that contain antibiotic resistance genes (ARGs) (Zhu et al., 2013; Widyasari-Mehta et al., 2016; Zhao et al., 2018). Previous studies have reported a significant increase in abundance and diversity of ARGs in soils following the application of pig manure (Heuer and Smalla, 2007; Zhu et al., 2013; Chen et al., 2017). However, no study has focused on the assessment of ARGs in nematode associated microbiomes. This may be critical for soil function as prior studies have shown that exposure to antibiotics could cause the accumulation of ARGs in honey bee (Tian et al., 2012) and collembolan gut microbiota (Zhu et al., 2018a), thus threatening the keystone position of nematodes in the soil food web.

As antimicrobial resistance is recognized as a serious and growing global problem (Zhu et al., 2013), many pig farms in China are amending their practice by reducing or halting the use of antibiotics to control the incidence and spread of ARGs. To ascertain the fate of ARGs in soil nematode communities, we compared pig manure with antibiotics in different levels. We hypothesize that 1) mineral fertilizer reduces the diversity of the nematode microbiome compared to the no fertilizer treatment, and 2) pig manure with the addition of antibiotics increases the abundance and diversity of ARGs in the nematode microbiome compared to other treatments.

To address these hypotheses, we established a microcosm experiment with four fertilization treatments. Our aims were to investigate the effects of fertilization on the nematode microbiome and further determine the abundance and composition of ARGs in the nematode microbiome by 16S rRNA gene high-throughput sequencing and high throughput quantitative PCR, and to explore the relationship between nematode associated microbial communities and their ARG profiles.

2. Materials and methods

2.1. Soil, plant and fertilizer

A sandy loam was collected from arable land used for a rice-wheat rotation near Ningbo China (29º 47′ N, 121º 21′ E). Samples were collected after harvesting rice (depth: 0-20 cm). After excluding large stones, root stubble and other debris, soil was gently sieved (5 mm, to maximize retention of soil nematodes) and mixed. The basic characteristics of the soil were: clay content = 7.35%, pH ($CaCl_2$) = 4.75, CEC = 13.76 cmol kg^{-1}, total C 32.4 g kg^{-1} and total N 3.77 g kg^{-1}. Wheat (cv. Yangmai 20, Ningbo Academy of Agricultural Sciences) seed was sterilized using 10% hydrogen peroxide for 15min and kept at 4 ºC for a week to ensure consistent germination prior to sowing.

Urea (CON_2H_4), superphosphate ($Ca(H_2PO_4)_2$) and potassium chloride (Sinopharm Chemical Reagent Co., Ltd, China) were used as inorganic fertilizers in our study. Organic fertilizers were two pig slurries obtained from a local farm: a dirty slurry (manure from pigs fed on fodder with added antibiotics) and a clean slurry (manure from pigs fed on fodder with a reduced antibiotic burden). The properties of

142 the dirty slurry were: total C = 218.9 mg kg^{-1}, total N = 28.9 mg kg^{-1}, ofloxacin = 0.021
143 mg kg^{-1} and oxytetracycline = 0.025 mg kg^{-1}, and the clean slurry: total C = 269.5 mg
144 kg^{-1}, total N = 33.6 mg kg^{-1}, ofloxacin = 0.003 mg kg^{-1} and oxytetracycline = 0.016 mg
145 kg^{-1}.

146 *2.2. Experimental design*

147 A greenhouse microcosm experiment was established with a replicated (n=3)
148 factorial design of four treatments: no fertilizer (NF), mineral fertilizer (MF), clean
149 slurry (CS) and dirty slurry (DS) to determine the effects of fertilization on nematode
150 microbiomes. The greenhouse temperature was set at 25 ^{o}C during the early growth
151 stages and at 20 ^{o}C for the late growth stages of wheat, ventilated and had natural
152 lighting. A total of 3 kg dried soil was transferred into individual polyvinyl chloride
153 pots (15 cm diameter, 23 cm height), and soil moisture adjusted to 60% to 70% of soil
154 water holding capacity. After pre-culture for a week, wheat seeds were sown and
155 fertilizer applied (70% of total fertilizer: 12.6 g N m^{-2}, 1.7 g P m^{-2} and 1.7 g K m^{-2}; no
156 fertilizer treatments: 0 g N m^{-2}, 1.7 g P m^{-2} and 1.7 g K m^{-2}) on the soil surface according
157 to local practice. Thereafter, 5.4 g N m^{-2}, 0.7 g P m^{-2} and 0.7 g K m^{-2} were applied
158 during the shoot-elongation growth stage. After three months of growth, wheat was
159 harvested, and soils from each pot were mixed well, and 600 g fresh soil sampled for
160 nematode extraction.

161 *2.3. Nematode extraction and DNA isolation*

The 600 g fresh soil was used to ensure that sufficient nematodes were obtained for the extraction of the nematode gut microbiome. A modified Baermann funnel was used to extract nematodes from 100 g soil sub-samples (Berg et al., 2016). Dominant individuals within the extracted communities were individually hand-picked using nippers under a dissecting microscope (SMZ-168) into anhydrous alcohol where they became moribund. Nematodes were then placed into 2% sodium hypochlorite solution for 10 s to avoid microbial contamination from their cuticle, then rinsed four times with aseptic phosphate buffer (Zhu et al, 2018a). The final wash buffer was spread on LB (Luria-Bertani) plates and incubated for 24 h. No colonies were observed on the plates suggesting that sterilization of the nematode cuticle had been achieved (Berg et al., 2016). Thereafter, nematodes were transferred into a 1.5 mL sterile centrifuge tube via sterile nippers under aseptic conditions, and stored at -20 ^{o}C until prior to DNA extraction.

DNA was extracted from approximately 100 nematodes per sample using a DNeasy Blood and Tissue Kit (QIAGEN, China (Shanghai) Co., Ltd). In brief, nematodes were homogenized in sterile 1.5-ml centrifuge tube using a micro-electric tissue homogenizer, and 20 ml proteinase K and 180 ml tissue lysis buffer (ATL) solution added to each tube. Tubes were vortexed for 60s and incubated at 56 °C for 8 hours. After incubation, the nematode DNA was extracted according to the kit manufacturer's instructions and frozen at -20 °C.

Nematode species identification was confirmed via the 5′ segment of the SSU barcode gene using primers: SSU18A (AAAGATTAAGCCA-TGCATG) and SSU26R (CATTCTTGGCAAATGCTTTCG) (Floyd et al., 2002). PCR products were ligated into a vector and transformed into *Escherichia coli* DH5α which was subsequently grown in 100 μL LB which was incubated on a shaking incubator at a speed of 200 rpm and temperature of 37 ^{o}C. Then an aliquot of liquid culture was spread onto plates which were incubated at 37 ^{o}C. After 12 h, three monoclonal colonies per sample were selected for sequencing. Sequences obtained were submitted to the National Center for Biotechnology Information (NCBI) using the Basic Local Alignment Search Tool (BLAST) and those assigned to *Dorylaimus stagnalis* which had a coverage of 92% over 99% nucleotides.

2.4 High-throughput quantitative PCR for analysis of ARGs

Extracted nematode DNA was used to detect the abundance and diversity of ARGs by high-throughput quantitative PCR reaction (SmartChip Real-time PCR Systems, Warfergen Inc., USA). A total of 296 primer sets targeting 285 ARGs, a 16S rRNA gene, a clinical class 1 integron, a class 1 integron and eight transposases (Table S1) were screened. Amplification of each primer set was replicated three times, and a non-template reaction was included as a negative control (Zhu et al., 2013; Ouyang et al., 2015). High throughput qPCR data were analysed using SmartChip qPCR software (V 2.7.0.1). Amplification efficiency varied between 90% and 110%. An amplification was regarded as successful when three positive replicates were observed. The detection

limit of amplification was set at a threshold cycle (C_T) of 31 (Zhu et al., 2013). To minimize error due to differences in 16S rRNA gene abundance between samples, a normalized copy number of ARGs per bacterial cell was used, calculated as follows (Ouyang et al., 2015; Zhu et al., 2018a):

$$\text{Relative ARG gene copy number} = 10^{(31-C_T)/(10/3)}$$

Normalized copy number of ARG gene = (Relative ARG gene copy number/ Relative 16S rRNA gene copy number) × 4.1.

Where C_T is the threshold value, 4.1 is the average number of 16S rRNA gene relative to a bacterial cell, which is estimated using the Ribosomal RNA Operon Copy Number Database (Klappenbach et al., 2001).

2.4. Sequencing library preparation and bioinformatics analysis

Universal bacterial primers (515F: GTGCCAGCMGCCGCGG and 907R: CCGTCAATCMTTTRAGTTT) equipped with unique barcodes were chosen to amplify (Zhu et al., 2018a; Zhu et al., 2018b) the bacterial 16S rRNA gene targeting hypervariable V4-V5 region (Turner et al., 1999). The concentration of purified products was determined using a Qubit 3.0 fluorimeter (Invitrogen, Ghent, Belgium). The library was obtained by pooling equal molar concentrations of each product and the library then run on the Illumina Hiseq2500 platform (Novogene, Tianjin, China).

The high-throughput sequencing data were analysed using Qiime v1.9.1 (Caporaso et al., 2010b). Post filtering the number of errors and reads length, removing

223 the low-quality reads, ambiguous nucleotides and barcodes and merging the raw pair-
224 end reads, clean sequences were clustered into operational taxonomic units (OTUs) at
225 97% sequence similarity (Edgar, 2010). Singletons were discarded, representative OTU
226 sequences aligned using PyNAST aligner (Caporaso et al., 2010a) and assigned
227 taxonomic status with RDP Classifier 2.2 using the bacterial database, Greengenes
228 v13.8 (McDonald et al., 2012; Langille et al., 2013). FastTree was used to produce the
229 phylogenetic tree (Price et al., 2010). The Shannon index was used to indicate bacterial
230 alpha diversity of OTUs. A principal coordinate analysis (PCoA) and a similarity
231 analysis (Anosim) were used to assess the difference in bacterial communities between
232 treatments. All high-throughput sequencing data were submitted to the NCBI Sequence
233 Read Archive under Bioproject PRJNA450154 and accession number SRP140547.

234 *2.5. Statistical analysis*

235 We used Microsoft Excel 2013 to calculate means and standard errors (SE) and
236 SPSS v20.0 to compare differences between treatments using one-way ANOVA test.
237 Pie graphs, column and scatter diagrams were produced using Origin 2017. Assembly
238 of the nematode microbiome used C-scores derived from soil nematode gut bacterial
239 co-occurrence patterns obtained by EcoSimR NulModels for Ecology in R (Castro-
240 Arellano et al., 2010; Berg et al., 2016). CoNet of Cytoscape 3.5.1 was used to construct
241 an interaction network and identify significant interactions (positive and negative)
242 between bacterial families that had a relative abundance >2% of the nematode
243 microbiome (Berg et al., 2016). The composition of microbial communities associated

with nematode and ARG profiles was determined using labdsv 1.8-0 within R (Roberts, 2012; RCoreTeam, 2017). A co-association network of nematode bacterial taxa and ARGs was produced using the R packages, psych and igraph (Csardi, 2006; Adair et al., 2018), and a heatmap (Kolde, 2015) of ARGs was drawn by the pheatmap package within R. Procrustes and Mantel tests within the Vegan 2.3-1 (Oksanen et al., 2017) package was used to explore the relationship between microbial communities associated with nematode and ARG profiles.

3. Results

3.1. Characterization of the nematode microbiome

A total of 984907 high quality sequences were identified, which were sorted into 63829 OTUs with at least 30249 sequences and 7805 OTUs in each sample. Proteobacteria (40.3%), Chloroflexi (13.7%), Firmicutes (12.3%), Actinobacteria (8.3%) and Acidobacteria (6.0%) were the five predominant bacterial phyla in soil nematode microbiomes (Figure S1). The dominant 15 bacterial families accounted for 47.9% of the total bacterial abundance (Figure S2), and the average abundance of each family across all samples was *ca.* 10%. The Shannon index of the nematode microbiome was 9.95 at a sequencing depth of 30249. The C-score suggested that the assembly of the nematode microbiome was not neutral in all samples (Figure S3). Interaction networks of the nematode microbiome showed that 205 positive and 204 negative interactions occurred, with more negative interactions associated with

264 *Spirobacillales* (52) and Burkholderiaceae (40) and more positive interactions with
265 Bacillaceae (27) and Xanthomonadaceae (27) (Figure S4).

266 *3.2. Effects of fertilization on the composition of the nematode microbiome*

267 Proteobacteria was the most abundant phylum in all treatments (no fertilizer:
268 38.9%, mineral fertilizer: 66.4%, clean slurry: 25.6% and dirty slurry: 30.1%).
269 Compared with no fertilizer, application of mineral fertilizer significantly increased the
270 relative abundance of Proteobacteria (by 70.1%; $P < 0.05$), and reduced the relative
271 abundance of Firmicutes (by 50.7%; $P < 0.05$) and Actinobacteria (by 48.4%; $P < 0.05$)
272 (Figure 1). No significant differences in the relative abundance of Proteobacteria,
273 Chloroflexi, Firmicutes and Actinobacteria were observed between organic fertilizers
274 (clean slurry and dirty slurry) and no fertilizer ($P > 0.05$), however, compared with no
275 fertilizer, clean slurry increased the proportion of Acidobacteria (ANOVA, $P < 0.05$;
276 Figure 1). At family level, compared with other treatments, higher abundance of
277 Spirobacillales (32.7%) occurred in the mineral fertilizer treatment (ANOVA, $P < 0.05$;
278 Figure S2). The total relative abundance of the dominant 15 bacterial families in the
279 mineral fertilizer treatment was significantly higher than that in other treatments
280 (ANOVA, $P < 0.001$; Figure S2).

281 *3.3. Effects of fertilization on the diversity of the nematode microbiome*

282 Application of fertilization significantly altered the bacterial community structure
283 of the nematode microbiome (PERMANOVA test, $P < 0.005$; Figure 2a). PCoA further
284 highlighted that the nematode microbiome from the mineral fertilizer treatment was

clustered separately from the other treatments in dimension 1 representing 56 % of the total variation, and the microbial community from the clean slurry was separated from treatments of no fertilizer and dirty slurry in the second dimension (explaining 12.7 % of the total variation) (Figure 2a). The diversity of the nematode microbiome in the mineral fertilizer treatment was significantly lower than the no fertilizer treatment, by 28.2% ($P < 0.05$; Figure 2b). In contrast, application of organic fertilizers (clean slurry and dirty slurry) did not significantly alter the diversity of the nematode microbiome compared to the no fertilizer treatment ($P > 0.05$; Figure 2b).

3.4. Effects of fertilization on the community assembly of the nematode microbiome

A null hypothesis model was used to assess the assemblage rules of the nematode microbial community using a Checkerboard score (C-score) from a co-occurrence analysis. C-score, which is an average number of instances of mutual exclusion in a set of communities, was calculated for nematode microbiota and compared with a distribution of scores produced via random permutations from the same data (Berg et al., 2016). The calculated C-score was distinct from the score distribution derived from a simulated metric (Figure S3) and thus the null hypothesis was rejected. This suggests that the community of the nematode microbiome was not neutral in all samples. Whilst, the assemblage of the nematode microbiome in the mineral fertilizer treatment was non-neutral, in contrast, the assembly was neutral in both the organic fertilizer treatments (Figure 3).

3.5. Effects of fertilization on ARGs profiles in the nematode microbiome

306 Across all samples, 72 ARGs, 1 transposase and 2 integrases were detected, and
307 divided into 9 categories (tetracycline, vancomycin, sulfonamide, beta-lactamase, other,
308 MLSB, multidrug, aminoglycoside and chloramphenicol) based on their recognized
309 resistance. The number of ARGs and mobile genetic elements (MGEs) ranged from 21
310 to 37 with no significant difference observed between treatments (ANOVA, $P > 0.05$;
311 Figure 4a). Similarly, there was no significant difference between treatments in the
312 normalized abundance of ARGs (ANOVA, $P > 0.05$; Figure 4b), although the highest
313 absolute abundance (2.71) was found in the mineral fertilizer treatment. However, the
314 PCoA of ARG profiles showed that the dirty slurry treatment clustered and separated
315 from the other treatments in dimension one representing 40% of total variation
316 (PERMANOVA test, $P < 0.01$; Figure 5a). Similarly, pheatmap analysis revealed that
317 the abundance of a number of ARGs, especially aminoglycoside and multidrug, was
318 increased in the organic fertilizer treatment (Figure 5b).

319 *3.6. Relationships between the nematode microbiome and ARG profiles*

320 A co-association network was constructed to explore the relationship between the
321 nematode microbiome (at family level > 2%) and ARGs. In total, 164 edges and 83
322 nodes were included in the co-association network, with a modularity of 0.6967 (Figure
323 6). No negative correlations were observed in the co-association network, and most
324 bacterial taxa (12/14) were connected with other bacteria and clustered together (Figure
325 6a), implying that the relationships between bacterial taxa and ARGs were limited and
326 weak. Procrustes analysis and Mantel test showed no significant correlation between

ARG profiles and nematode microbiomes (P > 0.85; Figure S8), which further supported a weak relationship. Four ARGs (oprD, mepA, mexF and mphA) were positively correlated with Thermogemmatisporaceae, and two ARGs (vanC and tetR) were positively correlated with Burkholderiaceae (Figure 6).

4. Discussion

4.1. The factors influencing the nematode microbiome

Our study showed that Proteobacteria was the dominant phylum in the microbiome of the soil nematode *D. stagnalis*, which concurs with previous studies on *C. elegans* (Berg et al., 2016; Dirksen et al., 2016) and nematodes extracted from marine sediment (Schuelke et al., 2018). However, Enterobacteriaceae has also been reported as a predominant bacterial family in the *C. elegans* microbiome (Berg et al., 2016; Dirksen et al., 2016), which differs from our results. Studies on nematode microbiomes are limited, so it is too soon to state whether variation exists between different nematode species (Schuelke et al., 2018) or populations of the same species. However, variations between different species or populations of the same species have been confirmed in many other taxa including fruit fly (Adair et al., 2018), water flea (Macke et al., 2017), collembolan (Bahrndorff et al., 2018) and honey bee (Kwong et al., 2017). In this study, the dominant 15 families accounted for only 47.9% of total bacterial abundance, suggesting a highly diverse microbial community inhabits nematodes, similar to that reported for collembolan (Zhu et al., 2018a) and earthworm (Pass et al., 2015). In contrast, only 8 families were identified in the gut of honey bees (Zheng et al., 2017).

348 The external environment plays a key role in shaping the microbiome (Wong et
349 al., 2015; Dirksen et al., 2016). Thus, diverse soil habitats may be an important factor
350 contributing to microbial diversity (Agamennone et al., 2015). Also, diet also has a vital
351 contribution to the host microbiome (Zhang et al., 2017). *D. stagnalis* is a large
352 omnivorous nematode, which is an indiscriminate feeder similar to earthworms and
353 contrast with honey bees that have a highly specialized feeding mechanism. The
354 assembly of the nematode microbiome was not neutral in all samples, with two of the
355 four treatments similar to that reported for the *C. elegans* microbiome (Berg et al., 2016).
356 An observed close connection between bacterial taxa was highlighted by the interaction
357 network, suggesting that competition and cooperation between bacterial members
358 frequently occurs in the nematode microbiome (Berg et al., 2016). This implies that
359 host niche formed from fertilizer pressure also has a potentially important role in
360 shaping the microbiome of *D. stagnalis*.

361 *4.2. Response of the D. stagnalis microbiome to fertilization*

362 Mineral fertilization significantly altered the composition and diversity of the
363 nematode microbiome. As animal-associated microbiomes can be beneficial to host
364 health and nutrient acquisition (Flint et al., 2012), a change in community composition
365 may affect nematode function (Li et al., 2010; Carrascosa et al., 2014). In this study,
366 the abundance of Proteobacteria was significantly increased in the nematode
367 microbiome in the mineral fertilizer treatment. Mineral fertilizer has been previously
368 reported to increase the relative abundance of Proteobacteria in soil microbial

communities (Dai et al., 2018), and environmental microorganisms have a contribution in shaping nematode gut microbiota (Berg et al., 2016). Thus, a shift in the soil microbial community may reflect the change of Proteobacteria in the nematode, which is supported by the increased relative abundance of Proteobacteria in soil with fertilization (Figure S5). It is well-known that an increase in the abundance of Proteobacteria often causes the dysbiosis of animal gut microbiota (Shin et al., 2015). Thus, application of mineral fertilizer may lead to an imbalanced gut microbiota in soil nematodes. Spirobacillales affliated to the order of deta-Proteobacteria comprises many pathogenic bacteria which may cause host inflammation (Brown and Peura, 1993). There is potential, therefore, that the high abundance of Spirobacillales detected in mineral fertilizer-treated soil nematodes, may have an impact on nematode health and function.

As we hypothesized, application of mineral fertilizer significantly reduced the diversity of the nematode microbiome. Three reasons may account for this reduced diversity: 1) Mineral fertilizer can affect the health of nematode (Paerl et al., 2014; Li et al., 2018), and host health has an essential influence on gut microbiota (Shapira, 2017); 2) Diet plays a crucial role in shaping host microbiomes (Hicks et al., 2018; Jehrke et al., 2018). Also, soil bacterial community diversity may be reduced by the application of mineral fertilizer (Dai et al., 2018), which could lead to a lower diversity of microorganisms accessible to nematodes. However, soil microbial community diversity in this experiment did not differ (Figures S6 and S7); and 3) Mineral fertilizer

390 can alter the soil environment (e.g. reduction of soil pH) (Dai et al., 2018), and changes
391 in the external environment may also affect the host microbiome. In addition, higher
392 microbial stability and better host health have been shown to be related to a greater
393 diversity of the host microbiome (Cotillard et al., 2013; Tap et al., 2015). Therefore,
394 these results indicate that application of mineral fertilizer may affect the health (and
395 function) of nematodes by reducing their microbial diversity, and vice versa.

396 In our study, application of organic fertilizers did not affect the diversity of the
397 nematode microbiome but altered the neutrality of its composition. Compared with
398 mineral fertilizer, organic fertilizers were more favorable to the nematode microbiome,
399 consistent with nematode community shifts under different fertilization treatments: no
400 fertilizer, organic manure, inorganic fertilizers and the combined applications of
401 manure with inorganic fertilizers (Li et al., 2010).

402 *4.3. Changes in ARG profile responded to fertilization*

403 Our results showed that whilst application of organic fertilizers did not increase
404 the total number or abundance of ARGs and MGEs in the nematode microbiome ($P >$
405 0.05), a number of ARGs were enriched in organic fertilizer treatments and ARG
406 profiles of the dirty slurry treatment were significantly different from the other
407 treatments. These results partly supported our hypothesis that organic fertilization
408 would increase the abundance and diversity of ARGs associated with the nematode
409 microbiome. Previous studies have shown organic fertilizers could substantially
410 increase ARGs in soil (Zhu et al., 2013; Chen et al., 2016). In this study, the enrichment

411 of many ARGs under organic fertilization indicated that ARGs can be transferred to
412 non-target soil nematodes. Previously in collembolan, we also observed that the
413 diversity and abundance of ARGs markedly increased in their gut microbiota due to
414 antibiotic exposure (Zhu et al., 2018a). This suggests that ARGs can enter the soil food
415 web and may generate a risk of ARG transfer along food chains.

416 In this study, although fertilization do not increase the total count of ARGs in the
417 nematode microbiome, and even co-association network and Procrustes analysis reveal
418 no significant relationship between the nematode microbiome and ARG profiles ($P >$
419 0.05), the abundance of most of ARGs (about 64%) was enriched in the organic
420 fertilizer treatments and diversity of ARGs was also increased, suggesting that there is
421 still a risk of horizontal gene transfer among nematode microbiome, which supports the
422 concept of the nematode gut being a potential refuge for ARGs. A similar phenomenon
423 was also observed in *Daphnia* (Eckert et al., 2016). Many previous studies also
424 illustrated that human and animal gut have an ability as a reservoir of ARGs due to a
425 niche of gut for diverse microbiota (Wang et al., 2016; Hu et al., 2017; Taft et al., 2018),
426 and organic fertilization caused the accumulation of resistome in earthworm gut
427 microbiome (Ding et al., 2019). Results reported here were based on only one
428 omnivorous nematode species. It is unknown whether these results would be common
429 to all nematode species from the full range of nematode functional groups (Yeates et
430 al., 1993). Thus, there is a clear imperative for future studies to address this knowledge
431 gap.

5. Conclusions

In conclusion, the microbiome of the nematode *D. stagnalis* is diverse, dominated by Proteobacteria and is not neutrally assembled. Application of mineral fertilizer significantly increased the abundance of Proteobacteria compared to the control and organic fertilization treatments and reduced the diversity of the nematode microbiome. In contrast, organic fertilizers had no impact on the composition or diversity of the nematode microbiome. Although some ARGs can be incorporated into the nematode microbiome from organic fertilizers, the total count and abundance of ARGs did not change, thus nematodes may be a refuge for ARGs. These results extend our knowledge on the effects of fertilization on soil-borne organisms and highlights that ARGs can be a component of field populations of the nematode microbiome.

Conflict of interest

The authors declare no competing financial interest.

Acknowledgments

This work was funded by the National Key R&D Program of China (2017YFE0107300), the National Natural Science Foundation of China (41571130063) and the Strategic Priority Research Program of the Chinese Academy of Sciences (XDB15020302 and XDB15020402). The James Hutton Institute receives financial support from the Scottish Government, Rural and Environment Science and Analytical Services Division.

References

Adair, K.L., Wilson, M., Bost, A., Douglas, A.E., 2018. Microbial community assembly in wild populations of the fruit fly *Drosophila melanogaster*. ISME J. 12, 959-972.

Agamennone, V., Jakupovic, D., Weedon, J.T., Suring, W.J., van Straalen, N.M., Roelofs, D., Roling, W.F.M., 2015. The microbiome of *Folsomia candida*: an assessment of bacterial diversity in a *Wolbachia*-containing animal. FEMS Microbiol. Ecol. 91(11), 1-10.

Bahrndorff, S., de Jonge, N., Hansen, J.K., Lauritzen, J.M.S., Spanggaard, L.H., Sorensen, M.H., Yde, M., Nielsen, J.L., 2018. Diversity and metabolic potential of the microbiota associated with a soil arthropod. Sci. Rep. 8, 2491-2498.

Berg, M., Stenuit, B., Ho, J., Wang, A., Parke, C., Knight, M., Alvarez-Cohen, L., Shapira, M., 2016. Assembly of the *Caenorhabditis elegans* gut microbiota from diverse soil microbial environments. ISME J. 10, 1998-2009.

Biederman, L.A., Boutton, T.W., Whisenant, S.G., 2008. Nematode community development early in ecological restoration: The role of organic amendments. Soil Biol. Biochem. 40, 2366-2374.

Boitt, G., Schmitt, D.E., Gatiboni, L.C., Wakelin, S.A., Black, A., Sacomori, W., Cassol, P.C., Condron, L.M., 2018. Fate of phosphorus applied to soil in pig slurry under cropping in southern Brazil. Geoderma 321, 164-172.

Boyle, E., 2017. Nitrogen pollution knows no bounds. Science 356, 700-701.

Brown, K.E., Peura, D.A., 1993. Diagnosis of *helicobacter-pylori* infection. Gastroenterol. Clin. N. 22, 105-115.

Caporaso, J.G., Bittinger, K., Bushman, F.D., DeSantis, T.Z., Andersen, G.L., Knight, R., 2010a. PyNAST: a flexible tool for aligning sequences to a template alignment. Bioinformatics 26, 266-267.

Caporaso, J.G., Kuczynski, J., Stombaugh, J., Bittinger, K., Bushman, F.D., Costello, E.K., Fierer, N., Pena, A.G., Goodrich, J.K., Gordon, J.I., Huttley, G.A., Kelley, S.T., Knights, D., Koenig, J.E., Ley, R.E., Lozupone, C.A., McDonald, D., Muegge, B.D., Pirrung, M., Reeder, J., Sevinsky, J.R., Tumbaugh, P.J., Walters, W.A., Widmann, J., Yatsunenko, T., Zaneveld, J., Knight, R., 2010b. QIIME allows analysis of high-throughput community sequencing data. Nat. Methods 7, 335-336.

Carrascosa, M., Sanchez-Moreno, S., Alonso-Prados, J.L., 2014. Relationships between nematode diversity, plant biomass, nutrient cycling and soil suppressiveness in fumigated soils. Eur. J. of Soil Biol. 62, 49-59.

Castro-Arellano, I., Lacher, T.E., Jr., Willig, M.R., Rangel, T.F., 2010. Assessment of assemblage-wide temporal niche segregation using null models. Methods Ecol. and Evol. 1, 311-318.

Chen, Q.L., An, X.L., Li, H., Su, J.Q., Ma, Y., Zhu, Y.G., 2016. Long-term field application of sewage sludge increases the abundance of antibiotic resistance genes in soil. Environ. Int. 92-93, 1-10.

Chen, Q.L., An, X.L., Li, H., Zhu, Y.G., Su, J.Q., Cui, L., 2017. Do manure-borne or indigenous soil microorganisms influence the spread of antibiotic resistance genes in manured soil? Soil Biol. Biochem. 114, 229-237.

Clark, L.C., Hodgkin, J., 2016. *Caenorhabditis* microbiota: worm guts get populated. BMC Biol. 14(37), 1-3.

Cotillard, A., Kennedy, S.P., Kong, L.C., Prifti, E., Pons, N., Le Chatelier, E., Almeida, M., Quinquis, B., Levenez, F., Galleron, N., Gougis, S., Rizkalla, S., Batto, J.-M., Renault, P., Dore, J., Zucker,

494 J.D., Clement, K., Ehrlich, S.D., Consortium, A.N.R.M., 2013. Dietary intervention impact on gut
495 microbial gene richness. Nature 500, 585.
496 Csardi, G., 2006. The igraph software package for complex network research. Inter J. Complex Syst.,
497 1695.
498 Cui, S., Shi, Y., Groffman, P.M., Schlesinger, W.H., Zhu, Y.G., 2013. Centennial-scale analysis of the
499 creation and fate of reactive nitrogen in China (1910-2010). Proc. Natl. Acad. Sci. U. S. A. 110,
500 2052-2057.
501 Dai, Z., Su, W., Chen, H., Barberan, A., Zhao, H., Yu, M., Yu, L., Brookes, P.C., Schadt, C.W., Chang,
502 S.X., Xu, J., 2018. Long-term nitrogen fertilization decreases bacterial diversity and favors the
503 growth of Actinobacteria and Proteobacteria in agro-ecosystems across the globe. Global Change
504 Biol. 24, 3452-3461.
505 Ding J., Zhu D., Hong B., Wang H.T., Li G., Ma Y.B., Tang Y.T., Chen Q.L., 2019. Long-term
506 application of organic fertilization causes the accumulation of antibiotic resistome in earthworm gut
507 microbiota. Environ. Int. 124, 145-152.
508 Dirksen, P., Marsh, S.A., Braker, I., Heitland, N., Wagner, S., Nakad, R., Mader, S., Petersen, C.,
509 Kowallik, V., Rosenstiel, P., Felix, M.A., Schulenburg, H., 2016. The native microbiome of the
510 nematode *Caenorhabditis elegans*: gateway to a new host-microbiome model. BMC Biol. 14(38),
511 1-16.
512 Eckert, E.M., Di Cesare, A., Stenzel, B., Fontaneto, D., Corno, G., 2016. *Daphnia* as a refuge for an
513 antibiotic resistance gene in an experimental freshwater community. Sci. Total Environ. 571, 77-81.
514 Edgar, R.C., 2010. Search and clustering orders of magnitude faster than BLAST. Bioinformatics 26,
515 2460-2461.
516 Ekschmitt, K., Bakonyi, G., Bongers, M., Bongers, T., Bostrom, S., Dogan, H., Harrison, A., Nagy, P.,
517 O'Donnell, A.G., Papatheodorou, E.M., Sohlenius, B., Stamou, G.P., Wolters, V., 2001. Nematode
518 community structure as indicator of soil functioning in European grassland soils. Eur. J. of Soil Biol.
519 37, 263-268.
520 Engel, P., Moran, N.A., 2013. The gut microbiota of insects - diversity in structure and function. FEMS
521 Microbiol. Rev. 37, 699-735.
522 Felix, M.A., Jovelin, R., Ferrari, C., Han, S., Cho, Y.R., Andersen, E.C., Cutter, A.D., Braendle, C., 2013.
523 Species richness, distribution and genetic diversity of *Caenorhabditis* nematodes in a remote
524 tropical rainforest. BMC Evol. Biol. 13(10), 1-13.
525 Ferris, H., Tuomisto, H., 2015. Unearthing the role of biological diversity in soil health. Soil Biol.
526 Biochem. 85, 101-109.
527 Flint, H.J., Scott, K.P., Louis, P., Duncan, S.H., 2012. The role of the gut microbiota in nutrition and
528 health. Nat. Rev. Gastroenterol. Hepatol. 9, 577-589.
529 Floyd, R., Abebe, E., Papert, A., Blaxter, M., 2002. Molecular barcodes for soil nematode identification.
530 Mol. Ecol. 11, 839-850.
531 Griffiths, B.S., Ball, B.C., Daniell, T.J., Hallett, P.D., Neilson, R., Wheatley, R.E., Osler, G., Bohanec,
532 M., 2010. Integrating soil quality changes to arable agricultural systems following organic matter
533 addition, or adoption of a ley-arable rotation. Appl. Soil Ecol. 46, 43-53.
534 Gross, L., 2006. Gut bacteria cospeciating with insects. PLoS Biol. 4, 357.

Haegeman, A., Vanholme, B., Jacob, J., Vandekerckhove, T.T.M., Claeys, M., Borgonie, G., Gheysen, G., 2009. An endosymbiotic bacterium in a plant-parasitic nematode: Member of a new *Wolbachia* supergroup. Int. J. Parasitol. 39, 1045-1054.

Heuer, H., Smalla, K., 2007. Manure and sulfadiazine synergistically increased bacterial antibiotic resistance in soil over at least two months. Environ. Microbiol. 9, 657-666.

Hicks, A.L., Lee, K.J., Couto-Rodriguez, M., Patel, J., Sinha, R., Guo, C., Olson, S.H., Seimon, A., Seimon, T.A., Ondzie, A.U., Karesh, W.B., Reed, P., Cameron, K.N., Lipkin, W.I., Williams, B.L., 2018. Gut microbiomes of wild great apes fluctuate seasonally in response to diet. Nat. Commun. 9, 1-18.

Hu Y.F., Gao G.F., Zhu B.L., 2017. The antibiotic resistome: gene flow in environments, animals and human beings. Front. Med. 11(2): 161-168.

Jehrke, L., Stewart, F.A., Droste, A., Beller, M., 2018. The impact of genome variation and diet on the metabolic phenotype and microbiome composition of *Drosophila melanogaster*. Sci. Rep. 8, 1-15.

Kautz, S., Rubin, B.E.R., Russell, J.A., Moreau, C.S., 2013. Surveying the microbiome of ants: comparing 454 pyrosequencing with traditional methods to uncover bacterial diversity. Appl. Environ. Microbiol. 79, 525-534.

Klappenbach, J.A., Saxman, P.R., Cole, J.R., Schmidt, T.M., 2001. rrndb: the ribosomal RNA operon copy number database. Nucleic Acids Res. 29, 181-184.

Kolde, R., 2015 pheatmap: Pretty Heatmaps. R package version 1.0.8; http://CRAN.R-project.org/package=pheatmap.

Kwong, W.K., Medina, L.A., Koch, H., Sing, K.W., Soh, E.J.Y., Ascher, J.S., Jaffe, R., Moran, N.A., 2017. Dynamic microbiome evolution in social bees. Sci. Adv. 3, 1600513.

Ladygina, N., Johansson, T., Canback, B., Tunlid, A., Hedlund, K., 2009. Diversity of bacteria associated with grassland soil nematodes of different feeding groups. FEMS Microbiol. Ecol. 69, 53-61.

Langille, M.G.I., Zaneveld, J., Caporaso, J.G., McDonald, D., Knights, D., Reyes, J.A., Clemente, J.C., Burkepile, D.E., Thurber, R.L.V., Knight, R., Beiko, R.G., Huttenhower, C., 2013. Predictive functional profiling of microbial communities using 16S rRNA marker gene sequences. Nat. Biotechnol. 31, 814.

Lazarova, S.S., Brown, D.J.F., Oliveira, C.M.G., Fenton, B., Mackenzie, K., Wright, F., Malloch, G., Neilson, R., 2016. Diversity of endosymbiont bacteria associated with a non-filarial nematode group. Nematology 18, 615-623.

Li, J., Wang, D., Fan, W., He, R., Yao, Y., Sun, L., Zhao, X., Wu, J., 2018. Comparative effects of different organic materials on nematode community in continuous soybean monoculture soil. Appl. Soil Ecol. 125, 12-17.

Li, Q., Jiang, Y., Liang, W., Lou, Y., Zhang, E., Liang, C., 2010. Long-term effect of fertility management on the soil nematode community in vegetable production under greenhouse conditions. Appl. Soil Ecol. 46, 111-118.

Ma, L., Li, B., Jiang, X.T., Wang, Y.L., Xia, Y., Li, A.D., Zhang, T., 2017. Catalogue of antibiotic resistome and host-tracking in drinking water deciphered by a large scale survey. Microbiome 5(1), 154.

Macke, E., Callens, M., De Meester, L., Decaestecker, E., 2017. Host-genotype dependent gut microbiota drives zooplankton tolerance to toxic cyanobacteria. Nat. Commun. 8, 1608.

McDonald, D., Price, M.N., Goodrich, J., Nawrocki, E.P., DeSantis, T.Z., Probst, A., Andersen, G.L., Knight, R., Hugenholtz, P., 2012. An improved Greengenes taxonomy with explicit ranks for ecological and evolutionary analyses of bacteria and archaea. ISME J. 6, 610-618.

Oksanen, J.; Blanchet, F. G.; Kindt, R.; Legendre, P.; Minchin, P. R.; O'Hara, R. B.; Simpson, G. L.; Solymos, P.; Steven, M. H. H.; Wagner, H., 2017. vegan: Community Ecology Package. R package version 2.4-3; http://CRAN.R-project.org/package=vegan.

Ouyang, W.Y., Huang, F.Y., Zhao, Y., Li, H., Su, J.Q., 2015. Increased levels of antibiotic resistance in urban stream of Jiulongjiang River, China. Appl. Microbiol. Biot. 99, 5697-5707.

Paerl, H.W., Gardner, W.S., McCarthy, M.J., Peierls, B.L., Wilhelm, S.W., 2014. Algal blooms: Noteworthy nitrogen. Science 346, 175-175.

Pan, F.; Han, X.; Li, N.; Yan, J.; Xu, Y., 2017. Effect of organic amendment amount on soil nematode community structure and metabolic footprints in Soybean Phase of Soybean-Maize Rotation in Mollisols. Pedosphere.

Pass, D.A., Morgan, A.J., Read, D.S., Field, D., Weightman, A.J., Kille, P., 2015. The effect of anthropogenic arsenic contamination on the earthworm microbiome. Environ. Microbiol. 17, 1884-1896.

Price, M.N., Dehal, P.S., Arkin, A.P., 2010. FastTree 2-approximately maximum-likelihood trees for large alignments. PLoS One 5, 9490.

RCoreTeam, 2017. A Language and Environment for Statistical Computing; R Foundation for Statistical Computing: Vienna, Austria; http://www.R-project.org.

Rizvi, A.N., Mehta, H.S., 2009. Significance of trophic diversity of soil nematodes. Ann. For. 17, 311-318.

Roberts, D. W., 2012. labdsv: Ordination and multivariate analysis for ecology.

Sauvadet, M., Chauvat, M., Cluzeau, D., Maron, P.-A., Villenave, C., Bertrand, I., 2016. The dynamics of soil micro-food web structure and functions vary according to litter quality. Soil Biol. Biochem. 95, 262-274.

Schuelke, T., Pereira, T.J., Hardy, S.M., Bik, H.M., 2018. Nematode-associated microbial taxa do not correlate with host phylogeny, geographic region or feeding morphology in marine sediment habitats. Mol. Ecol. 27, 1930-1951.

Sechi, V., De Goede, R.G.M., Rutgers, M., Brussaard, L., Mulder, C., 2018. Functional diversity in nematode communities across terrestrial ecosystems. Basic Appl. Ecol. 30, 76-86.

Shapira, M., 2017. Host-microbiota interactions in *Caenorhabditis elegans* and their significance. Curr. Opin. Microbiol. 38, 142-147.

Shin, N.R., Whon, T.W., Bae, J.W., 2015. Proteobacteria: microbial signature of dysbiosis in gut microbiota. Trends Biotechnol. 33, 496-503.

Sinnathamby, G., Henderson, G., Umair, S., Janssen, P., Bland, R., Simpson, H., 2018. The bacterial community associated with the sheep gastrointestinal nematode parasite *Haemonchus contortus*. PLoS One 13(2), 0192164.

Stagaman, K., Burns, A.R., Guillemin, K., Bohannan, B.J.M., 2017. The role of adaptive immunity as an ecological filter on the gut microbiota in zebrafish. ISME J. 11, 1630-1639.

Taft D.H., Liu J.X., Maldonado-Gomez M.X., Akre S, Huda M.N., Ahmad S.M., Stephensen C.B., Mills D.A., 2018. Bifidobacterial dominance of the gut in early life and acquisition of antimicrobial resistance. mSphere 3, 00441-18.

Tap, J., Furet, J.P., Bensaada, M., Philippe, C., Roth, H., Rabot, S., Lakhdari, O., Lombard, V., Henrissat, B., Corthier, G., Fontaine, E., Dore, J., Leclerc, M., 2015. Gut microbiota richness promotes its stability upon increased dietary fibre intake in healthy adults. Environ. Microbiol. 17, 4954-4964.

Tian, B., Fadhil, N.H., Powell, J.E., Kwong, W.K., Moran, N.A., 2012. Long-term exposure to antibiotics has caused accumulation of resistance determinants in the gut microbiota of honeybees. MBio 3(6), 377.

Turner, S., Pryer, K.M., Miao, V.P.W., Palmer, J.D., 1999. Investigating deep phylogenetic relationships among cyanobacteria and plastids by small submit rRNA sequence analysis. J. Eukaryot. Microbiol. 46, 327-338.

Wang H., Sangwan N., Li H.Y., Su J.Q., Ouyang W.Y., Zhang Z.J., Gilbert J.A., Zhu Y.G., Ping F., Zhang H.L., 2016. The antibiotic resistome of swine manure is significantly altered by association with the *Musca domestica* larvae gut microbiome. ISME J. 11, 100-111.

Widyasari-Mehta, A., Kartika, H.R., Suwito, A., Kreuzig, R., 2016. Laboratory testing on the removal of the veterinary antibiotic doxycycline during long-term liquid pig manure and digestate storage. Chemosphere 149, 154-160.

Wong, A.C., Luo, Y., Jing, X., Franzenburg, S., Bost, A., Douglas, A.E., 2015. The host as the driver of the microbiota in the gut and external environment of *Drosophila melanogaster*. Appl. Environ. Microbiol. 81, 6232-6240.

Wu, T.H., Edward, A., Richard, D.B., Wall, D.H., and James, R.G., 2011. Molecular study of worldwide distribution and diversity of soil animals. Proc. Natl. Acad. Sci. U. S. A. 108, 17720-17725.

Yeates, G.W., 2003. Nematodes as soil indicators: functional and biodiversity aspects. Biol. Fert. Soils 37, 199-210.

Yeates, G.W., Bongers, T., 1999. Nematode diversity in agroecosystems. Agr. Ecosyst. Environ. 74, 113-135.

Yeates, G.W., Bongers, T., de Goede, R.G.M., Freckman, D.W., Georgieva, S.S. 1993. Feeding habits in soil nematode families and genera - an outline for soil ecologists. J. Nematol. 25, 315-331.

Zhang, F., Berg, M., Dierking, K., Felix, M.A., Shapira, M., Samuel, B.S., Schulenburg, H., 2017. *Caenorhabditis elegans* as a model for microbiome research. Front. Microbiol. 8, 485-485.

Zhang, J.Y., Holdorf, A.D., Walhout, A.J.M., 2017. *C. elegans* and its bacterial diet as a model for systems-level understanding of host–microbiota interactions. Curr. Opin. Biotech. 46, 74-80.

Zhang, X., Guan, P., Wang, Y., Li, Q., Zhang, S., Zhang, Z., Bezemer, T.M., Liang, W., 2015. Community composition, diversity and metabolic footprints of soil nematodes in differently-aged temperate forests. Soil Biol. Biochem. 80, 118-126.

Zhao, Y., Su, J.Q., An, X.L., Huang, F.Y., Rensing, C., Brandt, K.K., Zhu, Y.G., 2018. Feed additives shift gut microbiota and enrich antibiotic resistance in swine gut. Sci. Total Environ. 621, 1224-1232.

Zheng, H., Powell, J.E., Steele, M.I., Dietrich, C., Moran, N.A., 2017. Honeybee gut microbiota promotes host weight gain via bacterial metabolism and hormonal signaling. Proc. Natl. Acad. Sci. U. S. A. 114, 4775-4780.

Zhu, D., An, X.L., Chen, Q.L., Yang, X.R., Christie, P., Ke, X., Wu, L.H., Zhu, Y.G., 2018a. Antibiotics disturb the microbiome and increase the incidence of resistance genes in the gut of a common soil collembolan. Environ. Sci. Technol. 52, 3081-3090.

Zhu, D., Chen, Q.L., An, X.L., Yang, X.R., Christie, P., Ke, X., Wu, L.H., Zhu, Y.G., 2018b. Exposure of soil collembolans to microplastics perturbs their gut microbiota and alters their isotopic composition. Soil Biol. Biochem. 116, 302-310.

Zhu, Y.G., Johnson, T.A., Su, J.Q., Qiao, M., Guo, G.X., Stedtfeld, R.D., Hashsham, S.A., Tiedje, J.M., 2013. Diverse and abundant antibiotic resistance genes in Chinese swine farms. Proc. Natl. Acad. Sci. U. S. A. 110, 3435-3440.

Figure legends

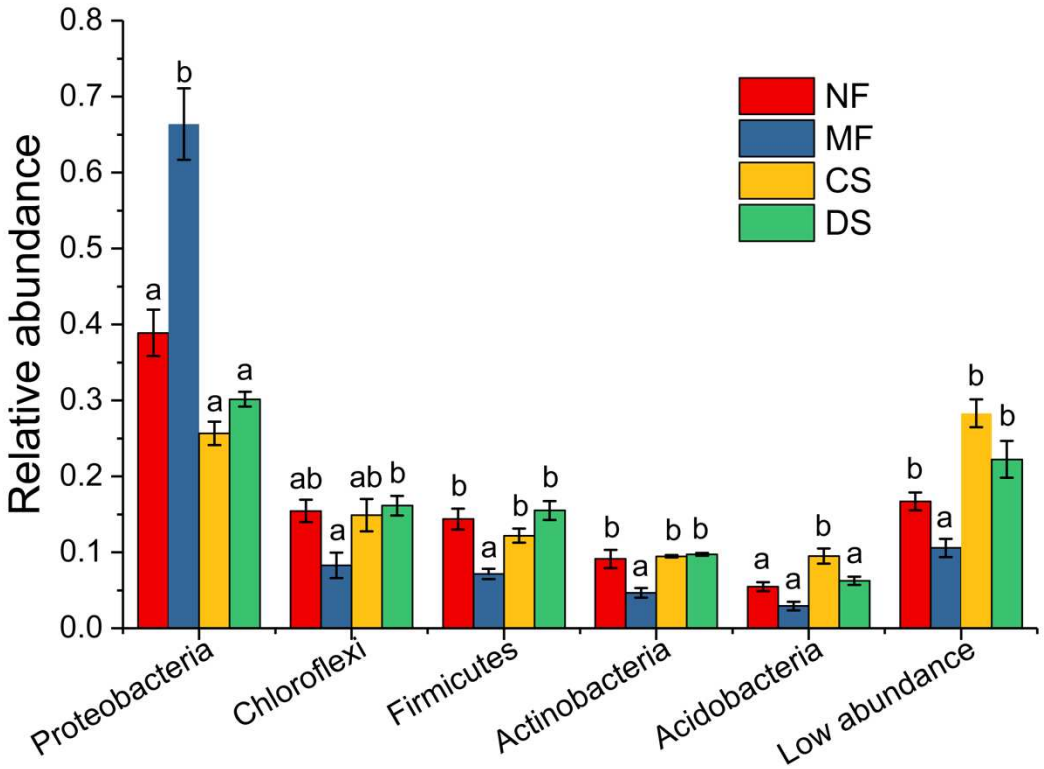

Figure 1. Relative abundance (mean ± SE, n = 3) of nematode microbiome at phylum level for all treatments ("NF", no fertilizer; "MF", mineral fertilizer; "CS", clean slurry; "DS", "dirty slurry"). "Low abundance" comprises of the relative abundance of phyla < 10%. Different letters indicate significant differences between treatments for each phylum at $P < 0.05$ (ANOVA).

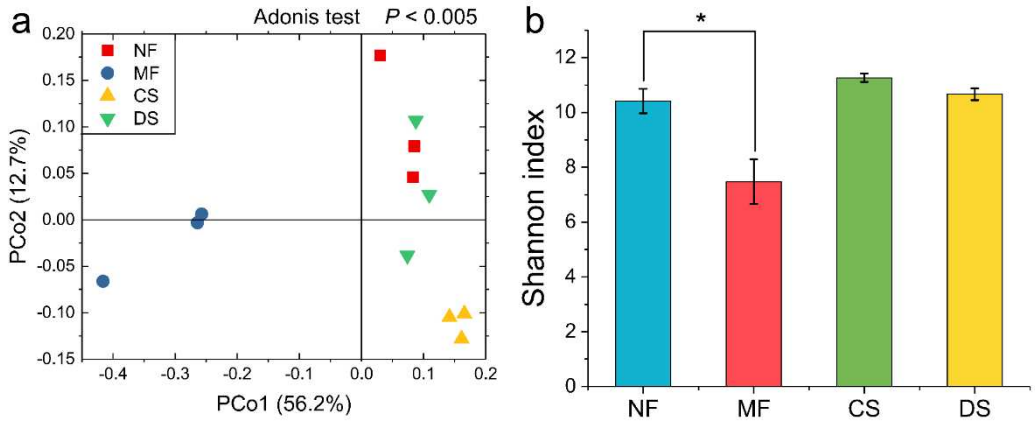

Figure 2. (a) Principal coordinates analysis (PCoA) of the nematode microbiome using relative abundance of OTUs based on Bray-Curtis distances. Treatments are indicated by different colours and shapes ("NF", no fertilizer; "MF", mineral fertilizer; "CS", clean slurry; "DS", "dirty slurry"). The explained variation is listed in parentheses. The Adonis test was used to compare the difference between treatments. (b) The Shannon index (mean ± SE, n = 3) of the nematode microbiome by treatment at a sequencing depth of 30249. The significant difference (ANOVA) between treatments is indicated by "*" (0.05 level).

692

693

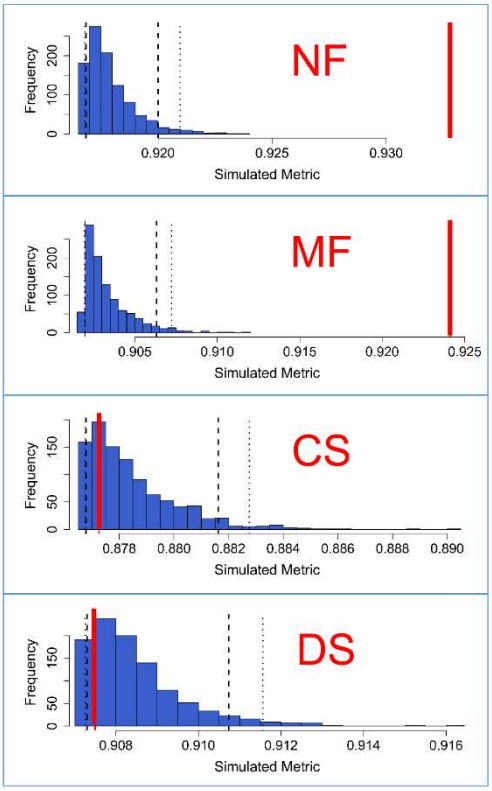

694

695 **Figure 3.** Assembly of the nematode microbiome in each treatment ("NF", no fertilizer;
696 "MF", mineral fertilizer; "CS", clean slurry; "DS", "dirty slurry"). C-score is an
697 estimation of the proportion of OUT pairs that have co-occurrence patterns and allows
698 measuring rules of microbial community assembly, with a random species assortment
699 as the null hypothesis. The C-score (red line) was calculated using the R package
700 "*bipartite*" from the abundant families of the soil nematode microbiome (relative
701 abundance > 0.5% and share ratio > 60% in nematode samples), compared with a
702 simulated metric generated from 5000 random permutations of the same data set (Blue

703 column). The long and short dashed line represents the 95% confidence interval for
704 one-tail and two-tail of hypothesis test, respectively.

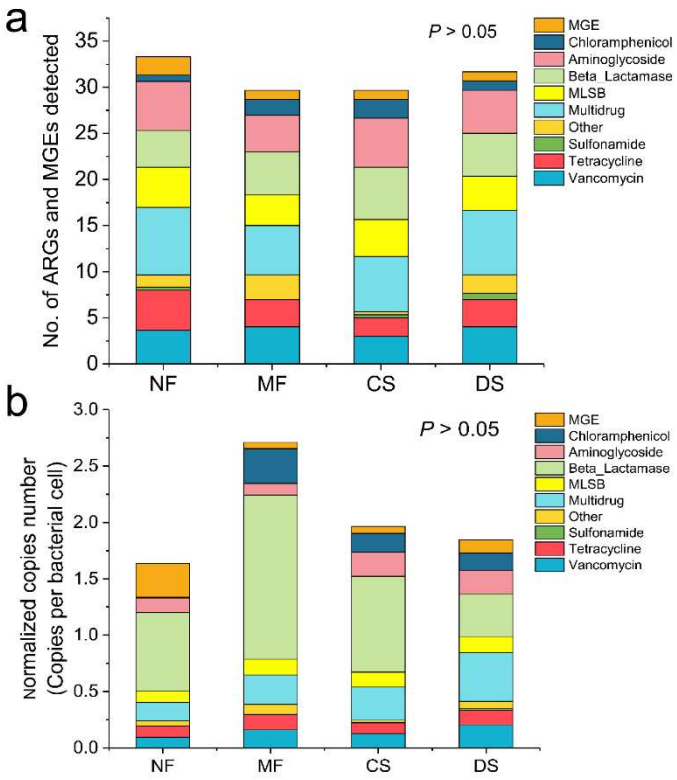

705

706 **Figure 4.** (a) Number and (b) abundance of detected ARGs and MGEs (mean ± SE, n
707 = 3) in each treatment ("NF", no fertilizer; "MF", mineral fertilizer; "CS", clean slurry;
708 "DS", "dirty slurry"). ARGs are classified according to their resistance. No significant
709 difference was found between treatments (ANOVA) at the 0.05 level.

710

711

712

713

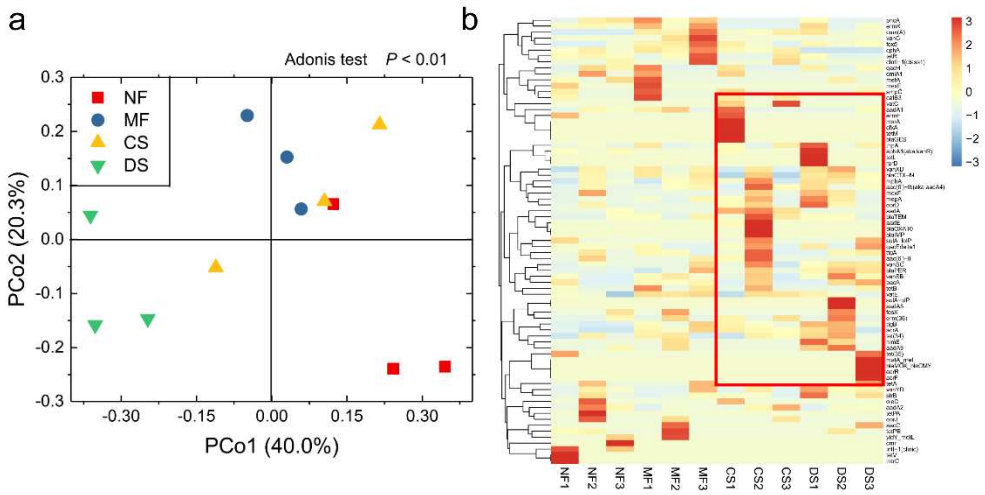

Figure 5. (a) Principal coordinates analysis (PCoA) of ARG profiles from soil nematode microbiomes based on Bray-Curtis distances. Different treatments are indicated by different colours and shapes ("NF", no fertilizer; "MF", mineral fertilizer; "CS", clean slurry; "DS", "dirty slurry"). The explained variation is listed in parentheses. The Adonis test was used to compare the difference between treatments. (b) Pheatmap depicting ARGs distribution profiles of the nematode microbiome in each treatment. The values of relative ARG abundance are transformed by the natural log for homoscedasticity. Those ARGs with enriched abundance due to the application of slurry are framed in red.

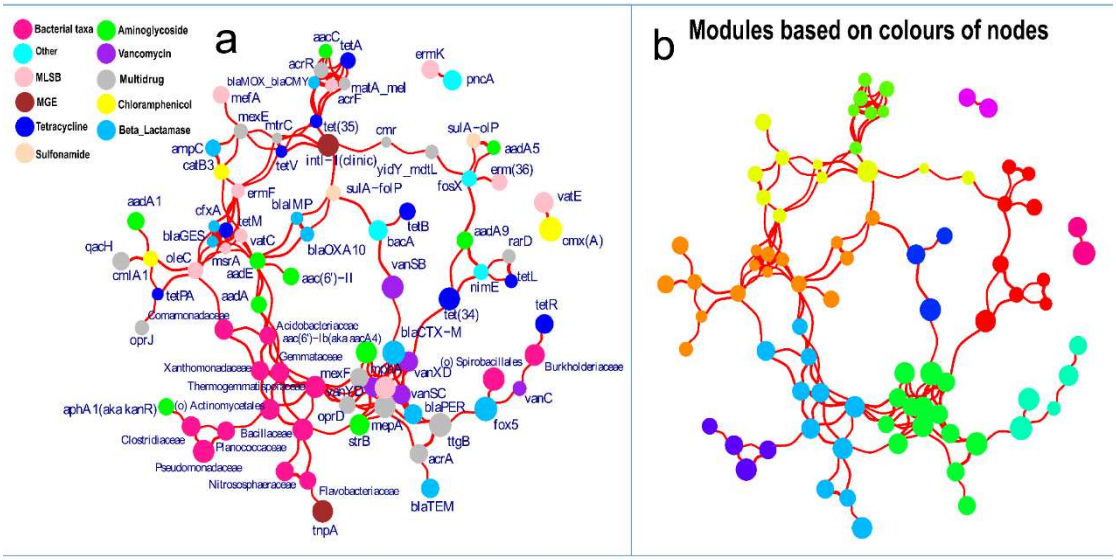

728

729 **Figure 6.** Co-association network of nematode microbiome (family with relative
730 abundance > 2%) and ARGs. Nodes represent bacterial taxa and ARGs, the size of each
731 node is proportional to its number of connections and red edges represent positive co-
732 associations (green edges representing negative co-associations, no negative in our
733 diagrams) and edge thickness indicates correlation coefficients. A connection
734 represents a strong (Spearman's rank correlation coefficient $\rho > 0.6$) and significant (P
735 value < 0.01) correlation. (a) Node colors represent bacterial taxa and antibiotic
736 resistance genes and node labels their names. (b) Modules based on node colors. The
737 high modularity index of 0.6967 implies that the entire network is parsed into 12
738 modules. The nodes inside modules are more correlated than that outside modules.

739

Supporting Information for

Mineral and organic fertilization alters the microbiome of a soil nematode *Dorylaimus stagnalis* and its resistome

Fei Zheng[a,b,#], Dong Zhu [a,b,#], Madeline Giles[c], Tim Daniell[c,d], Roy Neilson[c], Yong-Guan Zhu[a,b,e], Xiao-Ru Yang[a,*]

[a] *Key Laboratory of Urban Environment and Health, Institute of Urban Environment, Chinese Academy of Sciences, 1799 Jimei Road, Xiamen 361021, China.*

[b] *University of the Chinese Academy of Sciences, 19A Yuquan Road, Beijing 100049, China.*

[c] *Ecological Sciences, The James Hutton Institute, Dundee, DD2 5DA, Scotland, UK.*

[d] *Department of Animal and Plant Sciences, The University of Sheffield, Sheffield, S10 2TN, UK.*

[e] *State Key Laboratory of Urban and Regional Ecology, Research Center for Eco-Environmental Sciences, Chinese Academy of Sciences, Beijing 100085, China.*

[#] Fei Zheng and Dong Zhu contributed equally to this paper.

* Corresponding author: Xiao-Ru Yang

Key Laboratory of Urban Environment and Health, Institute of Urban Environment, Chinese Academy of Sciences, No.1799 Jimei Road, Xiamen 361021, China.

* E-mail address: xryang@iue.ac.cn. Tel: +86 592- 6190560; Fax: +86 592-6190977.

Contents

781 Bray−Curtis dissimilarity metrics (sum of squares M^2 = 0.9484, *P* = 0.8513, 9999

782 permutations).

783

784 **Total:**

785 **Number of tables: 1**

786 **Number of figures: 8**

787 **Number of pages: 34**

788 **Table S1:** Information of 296 genes detected in the gene chip.

Number	Gene Name	Forward Primer	Reverse Primer	Classification
1	16S rRNA	GGGTTGCGCTCGTTGC	ATGGYTGTCGTCAGCTCGTG	
2	aac	CCCTGCGTTGTGGCTATGT	TTGGCCACGCCAATCC	Aminoglycoside
3	aac(6')I1	GACCGGATTAAGGCCGATG	CTTGCCTTGATATTCAGTTTTTATAACCA	Aminoglycoside
4	aac(6')-Ib(aka aacA4)-01	GTTTGAGAGGCAAGGTACCGTAA	GAATGCCTGGCGTGTTTGA	Aminoglycoside
5	aac(6')-Ib(aka aacA4)-02	CGTCGCCGAGCAACTTG	CGGTACCTTGCCTCTCAAACC	Aminoglycoside
6	aac(6')-Ib(aka aacA4)-03	AGAAGCACGCCCGACACTT	GCTCTCCATTCAGCATTGCA	Aminoglycoside
7	aac(6')-II	CGACCCGACTCCGAACAA	GCACGAATCCTGCCTTCTCA	Aminoglycoside
8	aac(6')-Iy	GCTTTGCGGATGCCTCAAT	GGAGAACAAAAATACCTTCAAGGAAA	Aminoglycoside

9	aacA/aphD	AGAGCCTTGGGAAGATGAAGTTT	TTGATCCATACCATAGACTATCTCATCA	Aminoglycoside
10	aacC	CGTCACTTATTCGATGCCCTTAC	GTCGGGCGCGGCATA	Aminoglycoside
11	aacC1	GGTCGTGAGTTCGGAGACGTA	GCAAGTTCCCGAGGTAATCG	Aminoglycoside
12	aacC2	ACGGCATTCTCGATTGCTTT	CCGAGCTTCACGTAAGCATTT	Aminoglycoside
13	aacC4	CGGCGTGGGACACGAT	AGGGAACCTTTGCCATCAACT	Aminoglycoside
14	aadA-01	GTTGTGCACGACGACATCATT	GGCTCGAAGATACCTGCAAGAA	Aminoglycoside
15	aadA-02	CGAGATTCTCCGCGCTGTA	GCTGCCATTCTCCAAATTGC	Aminoglycoside
16	aadA1	AGCTAAGCGCGAACTGCAAT	TGGCTCGAAGATACCTGCAA	Aminoglycoside
17	aadA-1-01	AAAAGCCCGAAGAGGAACTTG	CATCTTTCACAAAGATGTTGCTGTCT	Aminoglycoside
18	aadA-1-02	CGGAATTGAAAAAACTGATCGAA	ATACCGGCTGTCCGTCATTT	Aminoglycoside

19	aadA2-01	ACGGCTCCGCAGTGGAT	GGCCACAGTAACCAACAAATCA	Aminoglycoside
20	aadA2-02	CTTGTCGTGCATGACGACATC	TCGAAGATACCCGCAAGAATG	Aminoglycoside
21	aadA2-03	CAATGACATTCTTGCGGGTATC	GACCTACCAAGGCAACGCTATG	Aminoglycoside
22	aadA5-01	ATCACGATCTTGCGATTTTGCT	CTGCGGATGGGCCTAGAAG	Aminoglycoside
23	aadA5-02	GTTCTTGCTCTTGCTCGCATT	GATGCTCGGCAGGCAAAC	Aminoglycoside
24	aadA9-01	CGCGGCAAGCCTATCTTG	CAAATCAGCGACCGCAGACT	Aminoglycoside
25	aadA9-02	GGATGCACGCTTGGATGAA	CCTCTAGCGGCCGGAGTATT	Aminoglycoside
26	aadD	CCGACAACATTTCTACCATCCTT	ACCGAAGCGCTCGTCGTATA	Aminoglycoside
27	aadE	TACCTTATTGCCCTTGGAAGAGTTA	GGAACTATGTCCCTTTTAATTCTACAATCT	Aminoglycoside
28	acrA-01	CAACGATCGGACGGGTTTC	TGGCGATGCCACCGTACT	Multidrug

29	acrA-02	GGTCTATCACCCTACGCGCTATC	GCGCGCACGAACATACC	Multidrug
30	acrA-03	CAGACCCGCATCGCATATT	CGACAATTTCGCGCTCATG	Multidrug
31	acrA-04	TACTTTGCGCGCCATCTTC	CGTGCGCGAACGAACAT	Multidrug
32	acrA-05	CGTGCGCGAACGAACA	ACTTTGCGCGCCATCTTC	Multidrug
33	acrB-01	AGTCGGTGTTCGCCGTTAAC	CAAGGAAACGAACGCAATACC	Multidrug
34	acrF	GCGGCCAGGCACAAAA	TACGCTCTTCCCACGGTTTC	Multidrug
35	acrR-01	GCGCTGGAGACACGACAAC	GCCTTGCTGCGAGAACAAA	Multidrug
36	acrR-02	GATGATACCCCCTGCTGTGAGA	ACCAAACAAGAAGCGCAAGAA	Multidrug
37	adeA	CAGTTCGAGCGCCTATTTCTG	CGCCCTGACCGACCAAT	Multidrug
38	ampC/blaDHA	TGGCCGCAGCAGAAAGA	CCGTTTTATGCACCCAGGAA	Beta_Lactamase

39	ampC-01	TGGCGTATCGGGTCAATGT	CTCCACGGGCCAGTTGAG	Beta_Lactamase
40	ampC-02	GCAGCACGCCCCGTAA	TGTACCCATGATGCGCGTACT	Beta_Lactamase
41	ampC-04	TCCGGTGACGCGACAGA	CAGCACGCCGGTGAAAGT	Beta_Lactamase
42	ampC-05	CTGTTCGAGCTGGGTTCTATAAGTAAA	CAGTATCTGGTCACCGGATCGT	Beta_Lactamase
43	ampC-06	CCGCTCAAGCTGGACCATAC	CCATATCCTGCACGTTGGTTT	Beta_Lactamase
44	ampC-07	CCGCCCAGAGCAAGGACTA	GCTCGACTTCACGCCGTAAG	Beta_Lactamase
45	ampC-09	CAGCCGCTGATGAAAAAATATG	CAGCGAGCCCACTTCGA	Beta_Lactamase
46	aph	TTTCAGCAAGTGGATCATGTTAAAAT	CCAAGCTGTTTCCACTGTTTTTC	Aminoglycoside
47	aph(2')-Id-01	TGAGCAGTATCATAAGTTGAGTGAAAAG	GACAGAACAATCAATCTCTATGGAATG	Aminoglycoside
48	aph(2')-Id-02	TAAGGATATACCGACAGTTTTGGAAA	TTTAATCCCTCTTCATACCAATCCATA	Aminoglycoside

49	aph6ia	CCCATCCCATGTGTAAGGAAA	GCCACCGCTTCTGCTGTAC	Aminoglycoside
50	aphA1(aka kanR)	TGAACAAGTCTGGAAAGAAATGCA	CCTATTAATTTCCCCTCGTCAAAAA	Aminoglycoside
51	bacA-01	CGGCTTCGTGACCTCGTT	ACAATGCGATACCAGGCAAAT	Others
52	bacA-02	TTCCACGACACGATTAAGTCATTG	CGGCTCTTTCGGCTTCAG	Others
53	bla1	GCAAGTTGAAGCGAAAGAAAAGA	TACCAGTATCAATCGCATATACACCTAA	Beta_Lactamase
54	bla-ACC-1	CACACAGCTGATGGCTTATCTAAAA	AATAAACGCGATGGGTTCCA	Beta_Lactamase
55	blaCMY	CCGCGGCGAAATTAAGC	GCCACTGTTTGCCTGTCAGTT	Beta_Lactamase
56	blaCMY2-01	AAAGCCTCAT GGGTGCATAAA	ATAGCTTTTGTTTGCCAGCATCA	Beta_Lactamase
57	blaCMY2-02	GCGAGCAGCCTGAAGCA	CGGATGGGCTTGTCCTCTT	Beta_Lactamase
58	blaCTX-M-01	GGAGGCGTGACGGCTTTT	TTCAGTGCGATCCAGACGAA	Beta_Lactamase

59	blaCTX-M-02	GCCGCGGTGCTGAAGA	ATCGGATTATAGTTAACCAGGTCAGATTT	Beta_Lactamase
60	blaCTX-M-03	CGATACCACCACGCCGTTA	GCATTGCCCAACGTCAGATT	Beta_Lactamase
61	blaCTX-M-04	CTTGGCGTTGCGCTGAT	CGTTCATCGGCACGGTAGA	Beta_Lactamase
62	blaCTX-M-05	GCGATAACGTGGCGATGAAT	GTCGAGACGGAACGTTTCGT	Beta_Lactamase
63	blaCTX-M-06	CACAGTTGGTGACGTGGCTTAA	CTCCGCTGCCGGTTTTATC	Beta_Lactamase
64	blaGES	GCAATGTGCTCAACGTTCAAG	GTGCCTGAGTCAATTCTTTCAAAG	Beta_Lactamase
65	blaIMP-01	AACACGGTTTGGTGGTTCTTGTA	GCGCTCCACAAACCAATTG	Beta_Lactamase
66	blaIMP-02	AAGGCAGCATTTCCTCTCATTTT	GGATAGATCGAGAATTAAGCCACTCT	Beta_Lactamase
67	bla-L1	CACCGGGTTACCAGCTGAAG	GCGAAGCTGCGCTTGTAGTC	Beta_Lactamase
68	blaMOX/blaCMY	CTATGTCAATGTGCCGAAGCA	GGCTTGTCCTCTTTCGAATAGC	Beta_Lactamase

69	blaOCH	GGCGACTTGCGCCGTAT	TTTTCTGCTCGGCCATGAG	Beta_Lactamase
70	blaOKP	GCCGCCATCACCATGAG	GGTGACGTTGTCACCGATCTG	Beta_Lactamase
71	blaOXA1/blaOXA30	CGGATGGTTTGAAGGGTTTATTAT	TCTTGGCTTTTATGCTTGATGTTAA	Beta_Lactamase
72	blaOXA10-01	CGCAATTATCGGCCTAGAAACT	TTGGCTTTCCGTCCCATTT	Beta_Lactamase
73	blaOXA10-02	CGCAATTATCGGCCTAGAAACT	TTGGCTTTCCGTCCCATTT	Beta_Lactamase
74	blaOXY	CGTTCAGGCGGCAGGTT	GCCGCGATATAAGATTTGAGAATT	Beta_Lactamase
75	blaPAO	CGCCGTACAACCGGTGAT	GAAGTAATGCGGTTCTCCTTTCA	Beta_Lactamase
76	blaPER	TGCTGGTTGCTGTTTTTGTGA	CCTGCGCAATGATAGCTTCAT	Beta_Lactamase
77	blaPSE	TTGTGACCTATTCCCCTGTAATAGAA	TGCGAAGCACGCATCATC	Beta_Lactamase
78	blaROB	GCAAAGGCATGACGATTGC	CGCGCTGTTGTCGCTAAA	Beta_Lactamase

79	blaSFO	CCGCCGCCATCCAGTA	GGGCCGCCAAGATGCT	Beta_Lactamase
80	blaSHV-01	TCCCATGATGAGCACCTTTAAA	TTCGTCACCGGCATCCA	Beta_Lactamase
81	blaSHV-02	CTTTCCCATGATGAGCACCTTT	TCCTGCTGGCGATAGTGGAT	Beta_Lactamase
82	blaTEM	AGCATCTTACGGATGGCATGA	TCCTCCGATCGTTGTCAGAAGT	Beta_Lactamase
83	blaTLA	ACACTTTGCCATTGCTGTTTATGT	TGCAAATTTCGGCAATAATCTTT	Beta_Lactamase
84	blaVEB	CCCGATGCAAAGCGTTATG	GAAAGATTCCCTTTATCTATCTCAGACAA	Beta_Lactamase
85	blaVIM	GCACTTCTCGCGGAGATTG	CGACGGTGATGCGTACGTT	Beta_Lactamase
86	blaZ	GGAGATAAAGTAACAAATCCAGTTAGATATGA	TGCTTAATTTTCCATTTGCGATAAG	Beta_Lactamase
87	carB	GGAGTGAGGCTGACCGTAGAAG	ATCGGCGAAACGCACAAA	MLSB
88	catA1	GGGTGAGTTTCACCAGTTTTGATT	CACCTTGTCGCCTTGCGTATA	Others

89	catB3	GCACTCGATGCCTTCCAAAA	AGAGCCGATCCAAACGTCAT	Others
90	catB8	CACTCGACGCCTTCCAAAG	CCGAGCCTATCCAGACATCATT	Others
91	ceoA	ATCAACACGGACCAGGACAAG	GGAAAGTCCGCTCACGATGA	Multidrug
92	cepA	AGTTGCGCAGAACAGTCCTCTT	TCGTATCTTGCCCGTCGATAAT	Beta_Lactamase
93	cfiA	GCAGCGTTGCTGGACACA	GTTCGGGATAAACGTGGTGACT	Beta_Lactamase
94	cfr	GCAAAATTCAGAGCAAGTTACGAA	AAAATGACTCCCAACCTGCTTTAT	Others
95	cfxA	TCATTCCTCGTTCAAGTTTTCAGA	TGCAGCACCAAGAGGAGATGT	Beta_Lactamase
96	cIntI-1(class1)	GGCATCCAAGCAGCAAG	AAGCAGACTTGACCTGA	Integron
97	cmeA	GCAGCAAAGAAGAAGCACCAA	AGCAGGGTAAGTAAAACTAAGTGGTAAATCT	Multidrug
98	cmlA1-01	TAGGAAGCATCGGAACGTTGAT	CAGACCGAGCACGACTGTTG	Chloramphenicol

99	cmlA1-02	AGGAAGCATCGGAACGTTGA	ACAGACCGAGCACGACTGTTG	Chloramphenicol
100	cmr	CGGCATCGTCAGTGGAATT	CGGTTCCGAAAAAGATGGAA	Multidrug
101	cmx(A)	GCGATCGCCATCCTCTGT	TCGACACGGAGCCTTGGT	Chloramphenicol
102	cphA-01	GCGAGCTGCACAAGCTGAT	CGGCCCAGTCGCTCTTC	Beta_Lactamase
103	cphA-02	GTGCTGATGGCGAGTTTCTG	GGTGTGGTAGTTGGTGTTGATCAC	Beta_Lactamase
104	dfrA1	GGAATGGCCCTGATATTCCA	AGTCTTGCGTCCAACCAACAG	Sulfonamide
105	dfrA12	CCTCTACCGAACCGTCACACA	GCGACAGCGTTGAAACAACTAC	Sulfonamide
106	emrD	CTCAGCAGTATGGTGGTAAGCATT	ACCAGGCGCCGAAGAAC	Multidrug
107	ereA	CCTGTGGTACGGAGAATTCATGT	ACCGCATTCGCTTTGCTT	MLSB
108	ereB	GCTTTATTTCAGGAGGCGGAAT	TTTTAAATGCCACAGCACAGAATC	Others

109	erm(34)	GCGCGTTGACGACGATTT	TGGTCATACTCGACGGCTAGAAC	MLSB
110	erm(35)	TTGAAAACGATGTTGCATTAAGTCA	TCTATAATCACAACTAACCACTTGAACGT	MLSB
111	erm(36)	GGCGGACCGACTTGCAT	TCTGCGTTGACGACGGTTAC	MLSB
112	ermA	TTGAGAAGGGATTTGCGAAAAG	ATATCCATCTCCACCATTAATAGTAAACC	MLSB
113	ermA/ermTR	ACATTTTACCAAGGAACTTGTGGAA	GTGGCATGACATAAACCTTCATCA	MLSB
114	ermB	TAAAGGGCATTTAACGACGAAACT	TTTATACCTCTGTTTGTTAGGGAATTGAA	MLSB
115	ermC	TTTGAAATCGGCTCAGGAAAA	ATGGTCTATTTCAATGGCAGTTACG	MLSB
116	ermF	CAGCTTTGGTTGAACATTTACGAA	AAATTCCTAAAATCACAACCGACAA	MLSB
117	ermJ/ermD	GGACTCGGCAATGGTCAGAA	CCCCGAAACGCAATATAATGTT	MLSB
118	ermK-01	GTTTGATATTGGCATTGTCAGAGAAA	ACCATTGCCGAGTCCACTTT	MLSB

119	ermK-02	GAGCCGCAAGCCCCTTT	GTGTTTCATTTGACGCGGAGTAA	MLSB
120	ermT-01	GTTCACTAGCACTATTTTTAATGACAGAAGT	GAAGGGTGTCTTTTTAATACAATTAACGA	MLSB
121	ermT-02	GTAAAATCCCTAGAGAATACTTTCATCCA	TGAGTGATATTTTTGAAGGGTGTCTT	MLSB
122	ermX	GCTCAGTGGTCCCCATGGT	ATCCCCCCGTCAACGTTT	MLSB
123	ermY	TTGTCTTTGAAAGTGAAGCAACAGT	TAACGCTAGAGAACGATTTGTATTGAG	MLSB
124	fabK	TTTCAGCTCAGCACTTTGGTCAT	AAGGCATCTTTTTCAGCCAGTTC	Others
125	floR	ATTGTCTTCACGGTGTCCGTTA	CCGCGATGTCGTCGAACT	Multidrug
126	folA	CGAGCAGTTCCTGCCAAAG	CCCAGTCATCCGGTTCATAATC	Sulfonamide
127	fosB	TCACTGTAACTAATGAAGCATTAGACCAT	CCATCTGGATCTGTAAAGTAAAGAGATC	Others
128	fosX	GATTAAGCCATATCACTTTAATTGTGAAAG	TCTCCTTCCATAATGCAAATCCA	Others

129	fox5	GGTTTGCCGCTGCAGTTC	GCGGCCAGGTGACCAA	Beta_Lactamase
130	imiR	CCGGACTAGAGCTTCATGTAAGC	CCCACGCGGTACTCTTGTAAA	Others
131	intI-1(clinic)	CGAACGAGTGGCGGAGGGTG	TACCCGAGAGCTTGGCACCCA	Integron
132	IS613	AGGTTCGGACTCAATGCAACA	TTCAGCACATACCGCCTTGAT	Transposase
133	lmrA-01	TCGACGTGACCGTAGTGAACA	CGTGACTACCCAGGTGAGTTGA	MLSB
134	lnuA-01	TGACGCTCAACACACTCAAAAA	TTCATGCTTAAGTTCCATACGTGAA	MLSB
135	lnuB-01	TGAACATAATCCCCTCGTTTAAAGAT	TAATTGCCCTGTTTCATCGTAAATAA	MLSB
136	lnuB-02	AAAGGAGAAGGTGACCAATACTCTGA	GGAGCTACGTCAAACAACCAGTT	MLSB
137	lnuC	TGGTCAATATAACAGATGTAAACCAGATTT	CACCCCAGCCACCATCAA	MLSB
138	marR-01	GCGGCGTACTGGTGAAGCTA	TGCCCTGGTCGTTGATGA	Multidrug

139	matA/mel	TAGTAGGCAAGCTCGGTGTTGA	CCTGTGCTATTTTAAGCCTTGTTTCT	MLSB
140	mdetl1	ATACAGCAGTGGATATTGGTTTAATTGT	TGCATAAGGTGAATGTTCCATGA	Multidrug
141	mdtA	CCTAACGGGCGTGACTTCA	TTCACCTGTTTCAAGGGTCAAA	MLSB
142	mdtE/yhiU	CGTCGGCGCACTCGTT	TCCAGACGTTGTACGGTAACCA	Multidrug
143	mecA	GGTTACGGACAAGGTGAAATACTGAT	TGTCTTTTAATAAGTGAGGTGCGTTAATA	Beta_Lactamase
144	mefA	CCGTAGCATTGGAACAGCTTTT	AAACGGAGTATAAGAGTGCTGCAA	MLSB
145	mepA	ATCGGTCGCTCTTCGTTCAC	ATAAATAGGATCGAGCTGCTGGAT	Multidrug
146	mexA	AGGACAACGCTATGCAACGAA	CCGGAAAGGGCCGAAAT	Multidrug
147	mexD	TTGCCACTGGCTTTCATGAG	CACTGCGGAGAACTGTCTGTAGA	Multidrug
148	mexE	GGTCAGCACCGACAAGGTCTAC	AGCTCGACGTACTTGAGGAACAC	Multidrug

149	mexF	CCGCGAGAAGGCCAAGA	TTGAGTTCGGCGGTGATGA	Multidrug
150	mphA-01	CTGACGCGCTCCGTGTT	GGTGGTGCATGGCGATCT	MLSB
151	mphA-02	TGATGACCCTGCCATCGA	TTCGCGAGCCCCTCTTC	MLSB
152	mphB	CGCAGCGCTTGATCTTGTAG	TTACTGCATCCATACGCTGCTT	MLSB
153	mphC	CGTTTGAAGTACCGAATTGGAAA	GCTGCGGGTTTGCCTGTA	MLSB
154	msrA-01	CTGCTAACACAAGTACGATTCCAAAT	TCAAGTAAAGTTGTCTTACCTACACCATT	MLSB
155	msrC-01	TCAGACCGGATCGGTTGTC	CCTATTTTTTGGAGTCTTCTCTCTAATGTT	MLSB
156	mtrC-01	GGACGGGAAGATGGTCCAA	CGTAGCGTTCCGGTTCGAT	Multidrug
157	mtrC-02	CGGAGTCCATCGACCATTTG	ATCGTCGGCAAGGAGAATCA	Multidrug
158	mtrD-02	GGTCGGCACGCTCTTGTC	TGAAGAATTTGCGCACCACTAC	Multidrug

159	mtrD-03	CCGCCAAGCCGATATAGACA	GGCCGGGTTGCCAAA	Multidrug
160	ndm-1	ATTAGCCGCTGCATTGAT	CATGTCGAGATAGGAAGTG	Beta_Lactamase
161	nimE	TGCGCCAAGATAGGGCATA	GTCGTGAATTCGGCAGGTTTA	Others
162	nisB	GGGAGAGTTGCCGATGTTGTA	AGCCACTCGTTAAAGGGCAAT	Others
163	oleC	CCCGGAGTCGATGTTCGA	GCCGAAGACGTACACGAACAG	MLSB
164	oprD	ATGAAGTGGAGCGCCATTG	GGCCACGGCGAACTGA	Multidrug
165	oprJ	ACGAGAGTGGCGTCGACAA	AAGGCGATCTCGTTGAGGAA	Multidrug
166	pbp	CCGGTGCCATTGGTTTAGA	AAAATAGCCGCCCCAAGATT	Beta_Lactamase
167	pbp2x	TTTCATAAGTATCTGGACATGGAAGAA	CCAAAGGAAACTTGCTTGAGATTAG	Beta_Lactamase
168	Pbp5	GGCGAACTTCTAATTAATCCTATCCA	CGCCGATGACATTCTTCTTATCTT	Beta_Lactamase

169	penA	AGACGGTAACGTATAACTTTTTGAAAGA	GCGTGTAGCCGGCAATG	Beta_Lactamase
170	pikR1	TCGACATGCGTGACGAGATT	CCGCGAATTAGGCCAGAA	MLSB
171	pikR2	TCGTGGGCCAGGTGAAGA	TTCCCCTTGCCGGTGAA	MLSB
172	pmrA	TTTGCAGGTTTTGTTCCTAATGC	GCAGAGCCTGATTTCTCCTTTG	Multidrug
173	pncA	GCAATCGAGGCGGTGTTC	TTGCCGCAGCCAATTCA	Others
174	putitive multidrug	AATTTTGCCGATTATTGCTGAAA	GATTGTCATCATTCGTTTATCACCAA	Multidrug
175	qac	CAATAATAACCGAAATAATAGGGACAAGTT	AATAAGTGTTCCTAGTGTTGGCCATAG	Multidrug
176	qacA	TGGCAATAGGAGCTATGGTGTTT	AAGGTAACACTATTTTCGGTCCAAATC	Multidrug
177	qacA/qacB	TTTAGGCAGCCTCGCTTCA	CCGAATCCAAATAAAACCCAATAA	Multidrug
178	qacEdelta1-01	TCGCAACATCCGCATTAAAA	ATGGATTTCAGAACCAGAGAAAGAAA	Multidrug

179	qacEdelta1-02	CCCCTTCCGCCGTTGT	CGACCAGACTGCATAAGCAACA	Multidrug
180	qacH-01	GTGGCAGCTATCGCTTGGAT	CCAACGAACGCCCACAA	Multidrug
181	qacH-02	CATCGTGCTTGTGGCAGCTA	TGAACGCCCAGAAGTCTAGTTTT	Multidrug
182	qnrA	AGGATTTCTCACGCCAGGATT	CCGCTTTCAATGAAACTGCAA	Others
183	rarD-02	TGACGCATCGCGTGATCT	AAATTTTCTGTGGCGTCTGAATC	Multidrug
184	sat4	GAATGGGCAAAGCATAAAAACTTG	CCGATTTTGAAACCACAATTATGATA	Others
185	sdeB	CACTACCGCTTCCGCACTTAA	TGAAAAAACGGGAAAAGTCCAT	Multidrug
186	spcN-01	AAAAGTTCGATGAAACACGCCTAT	TCCAGTGGTAGTCCCCGAATC	Aminoglycoside
187	spcN-02	CAGAATCTTCCTGAAAAGTTTGATGAA	CGCAGACACGCCGAATC	Aminoglycoside
188	speA	GCAAGAGGTATTTGCTCAACAAGA	CAGGGTCACCCTCATAAAGAAAA	Others

189	str	AATGAGTTTTGGAGTGTCTCAACGTA	AATCAAAACCCCTATTAAAGCCAAT	Aminoglycoside
190	strA	CCGGTGGCATTTGAGAAAAA	GTGGCTCAACCTGCGAAAAG	Aminoglycoside
191	strB	GCTCGGTCGTGAGAACAATCT	CAATTTCGGTCGCCTGGTAGT	Aminoglycoside
192	sul1	CAGCGCTATGCGCTCAAG	ATCCCGCTGCGCTGAGT	Sulfonamide
193	sul2	TCATCTGCCAAACTCGTCGTTA	GTCAAAGAACGCCGCAATGT	Sulfonamide
194	sulA/folP-01	CAGGCTCGTAAATTGATAGCAGAAG	CTTTCCTTGCGAATCGCTTT	Sulfonamide
195	sulA/folP-03	CACGGCTTCGGCTCATGT	TGCCATCCTGTGACTAGCTACGT	Sulfonamide
196	tet(32)	CCATTACTTCGGACAACGGTAGA	CAATCTCTGTGAGGGCATTTAACA	Tetracycline
197	tet(34)	CTTAGCGCAAACAGCAATCAGT	CGGTGATACAGCGCGTAAACT	Tetracycline
198	tet(35)	ACCCCATGACGTACCTGTAGAGA	CAACCCACACTGGCTACCAGTT	Tetracycline

199	tet(36)-01	AGAATACTCAGCAGAGGTCAGTTCCT	TGGTAGGTCGATAACCCGAAAAT	Tetracycline
200	tet(36)-02	TGCAGGAAAGACCTCCATTACAG	CTTTGTCCACACTTCCACGTACTATG	Tetracycline
201	tet(37)	GAGAACGTTGAAAAGGTGGTGAA	AACCAAGCCTGGATCAGTCTCA	Tetracycline
202	tetA-01	GCTGTTTGTTCTGCCGGAAA	GGTTAAGTTCCTTGAACGCAAACT	Tetracycline
203	tetA-02	CTCACCAGCCTGACCTCGAT	CACGTTGTTATAGAAGCCGCATAG	Tetracycline
204	tetB-01	AGTGCGCTTTGGATGCTGTA	AGCCCCAGTAGCTCCTGTGA	Tetracycline
205	tetB-02	GCCCAGTGCTGTTGTTGTCAT	TGAAAGCAAACGGCCTAAATACA	Tetracycline
206	tetC-01	CATATCGCAATACATGCGAAAAA	AAAGCCGCGGTAAATAGCAA	Tetracycline
207	tetC-02	ACTGGTAAGGTAAACGCCATTGTC	ATGCATAAACCAGCCATTGAGTAAG	Tetracycline
208	tetD-01	TGCCGCGTTTGATTACACA	CACCAGTGATCCCGGAGATAA	Tetracycline

209	tetD-02	TGTCATCGCGCTGGTGATT	CATCCGCTTCCGGGAGAT	Tetracycline
210	tetE	TTGGCGCTGTATGCAATGAT	CGACGACCTATGCGATCTGA	Tetracycline
211	tetG-01	TCAACCATTGCCGATTCGA	TGGCCCGGCAATCATG	Tetracycline
212	tetG-02	CATCAGCGCCGGTCTTATG	CCCCATGTAGCCGAACCA	Tetracycline
213	tetH	TTTGGGTCATCTTACCAGCATTAA	TTGCGCATTATCATCGACAGA	Tetracycline
214	tetJ	GGGTGCCGCATTAGATTACCT	TCGTCCAATGTAGAGCATCCATA	Tetracycline
215	tetK	CAGCAGTCATTGGAAAATTATCTGATTATA	CCTTGTACTAACCTACCAAAAATCAAAATA	Tetracycline
216	tetL-01	AGCCCGATTTATTCAAGGAATTG	CAAATGCTTTCCCCCTGTTCT	Tetracycline
217	tetL-02	ATGGTTGTAGTTGCGCGCTATAT	ATCGCTGGACCGACTCCTT	Tetracycline
218	tetM-01	CATCATAGACACGCCAGGACATAT	CGCCATCTTTTGCAGAAATCA	Tetracycline

219	tetM-02	TAATATTGGAGTTTTAGCTCATGTTGATG	CCTCTCTGACGTTCTAAAAGCGTATTAT	Tetracycline
220	tetO-01	ATGTGGATACTACAACGCATGAGATT	TGCCTCCACATGATATTTTTCCT	Tetracycline
221	tetPA	AGTTGCAGATGTGTATAGTCGTAAACTATCTATT	TGCTACAAGTACGAAAACAAAACTAGAA	Tetracycline
222	tetPB-01	ACACCTGGACACGCTGATTTT	ACCGTCTAGAACGCGGAATG	Tetracycline
223	tetPB-02	TGATACACCTGGACACGCTGAT	CGTCCAAAACGCGGAATG	Tetracycline
224	tetPB-03	TGGGCGACAGTAGGCTTAGAA	TGACCCTACTGAAACATTAGAAATATACCT	Tetracycline
225	tetPB-04	AGTGGTGCAAATACTGAAAAAGTTGT	TTTGTTCCTTCGTTTTGGACAGA	Tetracycline
226	tetPB-05	CTGAAGTGGAGCGATCATTCC	CCCTCAACGGCAGAAATAACTAA	Tetracycline
227	tetQ	CGCCTCAGAAGTAAGTTCATACACTAAG	TCGTTCATGCGGATATTATCAGAAT	Tetracycline
228	tetR-02	CGCGATAGACGCCTTCGA	TCCTGACAACGAGCCTCCTT	Tetracycline

229	tetR-03	CGCGATGGAGCAAAAGTACAT	AGTGAAAAACCTTGTTGGCATAAAA	Tetracycline
230	tetS	TTAAGGACAAACTTTCTGACGACATC	TGTCTCCCATTGTTCTGGTTCA	Tetracycline
231	tetT	CCATATAGAGGTTCCACCAAATCC	TGACCCTATTGGTAGTGGTTCTATTG	Tetracycline
232	tetU-01	GTGGCAAAGCAACGGATTG	TGCGGGCTTGCAAAACTATC	Tetracycline
233	tetV	GCGGGAACGACGATGTATATC	CCGCTATCTCACGACCATGAT	Tetracycline
234	tetX	AAATTTGTTACCGACACGGAAGTT	CATAGCTGAAAAAATCCAGGACAGTT	Tetracycline
235	tnpA-01	CATCATCGGACGGACAGAATT	GTCGGAGATGTGGGTGTAGAAAGT	Transposase
236	tnpA-02	GGGCGGGTCGATTGAAA	GTGGGCGGGATCTGCTT	Transposase
237	tnpA-03	AATTGATGCGGACGGCTTAA	TCACCAAACTGTTTATGGAGTCGTT	Transposase
238	tnpA-04	CCGATCACGGAAAGCTCAAG	GGCTCGCATGACTTCGAATC	Transposase

239	tnpA-05	GCCGCACTGTCGATTTTTATC	GCGGGATCTGCCACTTCTT	Transposase
240	tnpA-07	GAAACCGATGCTACAATATCCAATTT	CAGCACCGTTTGCAGTGTAAG	Transposase
241	tolC-01	GGCCGAGAACCTGATGCA	AGACTTACGCAATTCCGGGTTA	Multidrug
242	tolC-02	CAGGCAGAGAACCTGATGCA	CGCAATTCCGGGTTGCT	Multidrug
243	tolC-03	GCCAGGCAGAGAACCTGATG	CGCAATTCCGGGTTGCT	Multidrug
244	Tp614	GGAAATCAACGGCATCCAGTT	CATCCATGCGCTTTTGTCTCT	Transposase
245	ttgA	ACGCCAATGCCAAACGATT	GTCACGGCGCAGCTTGA	Multidrug
246	ttgB	TCGCCCTGGATGTACACCTT	ACCATTGCCGACATCAACAAC	Multidrug
247	vanA	AAAAGGCTCTGAAAACGCAGTTAT	CGGCCGTTATCTTGTAAAAACAT	Vancomycin
248	vanB-01	TTGTCGGCGAAGTGGATCA	AGCCTTTTTCCGGCTCGTT	Vancomycin

249	vanB-02	CCGGTCGAGGAACGAAATC	TCCTCCTGCAAAAAAAGATCAAC	Vancomycin
250	vanC-01	ACAGGGATTGGCTATGAACCAT	TGACTGGCGATGATTTGACTATG	Vancomycin
251	vanC-03	AAATCAATACTATGCCGGGCTTT	CCGACCGCTGCCATCA	Vancomycin
252	vanC1	AGGCGATAGCGGGTATTGAA	CAATCGTCAATTGCTCATTTCC	Vancomycin
253	vanC2/vanC3	TTTGACTGTCGGTGCTTGTGA	TCAATCGTTTCAGGCAATGG	Vancomycin
254	vanG	ATTTGAATTGGCAGGTATACAGGTTA	TGATTTGTCTTTGTCCATACATAATGC	Vancomycin
255	vanHB	GAGGTTTCCGAGGCGACAA	CTCTCGGCGGCAGTCGTAT	Vancomycin
256	vanHD	GTGGCCGATTATACCGTCATG	CGCAGGTCATTCAGGCAAT	Vancomycin
257	vanRA-01	CCCTTACTCCCACCGAGTTTT	TTCGTCGCCCCATATCTCAT	Vancomycin
258	vanRA-02	CCACTCCGGCCTTGTCATT	GCTAACCACATTCCCCTTGTTTT	Vancomycin

259	vanRB	GCCCTGTCGGATGACGAA	TTACATAGTCGTCTGCCTCTGCAT	Vancomycin
260	vanRC	TGCGGGAAAAACTGAACGA	CCCCCCATACGGTTTTGATTA	Vancomycin
261	vanRC4	AGTGCTTTGGCTTATCTCGAAAA	TCCGGCAGCATCACATCTAA	Vancomycin
262	vanRD	TTATAATGGCAAGGATGCACTAAAGT	CGTCTACATCCGGAAGCATGA	Vancomycin
263	vanSA	CGCGTCATGCTTTCAAAATTC	TCCGCAGAAAGCTCAATTTGTT	Vancomycin
264	vanSB	GCGCGGCAAATGACAAC	TTTGCCATTTTATTCGCACTGT	Vancomycin
265	vanSC-02	GCCATCAGCGAGTCTGATGA	CAGCTGGGATCGTTTTTCCTT	Vancomycin
266	vanSE	TGGCCGAAGAAGCAGGAA	CAATAATACTCGTCAAAGGAGTTCTCA	Vancomycin
267	vanTC-01	CACACGCATTTTTTCCCATCTAG	CAGCCAACAGATCATCAAAACAA	Vancomycin
268	vanTC-02	ACAGTTGCCGCTGGTGAAG	CGTGGCTGGTCGATCAAAA	Vancomycin

269	vanTE	GTGGTGCCAAGGAAGTTGCT	CGTAGCCACCGCAAAAAAAT	Vancomycin
270	vanTG	CGTGTAGCCGTTCCGTTCTT	CGGCATTACAGGTATATCTGGAAA	Vancomycin
271	vanWB	CGGACAAAGATACCCCCTATAAAG	AAATAGTAAATTGCTCATCTGGCACAT	Vancomycin
272	vanWG	ACATTTTCATTTTGGCAGCTTGTAC	CCGCCATAAGAGCCTACAATCT	Vancomycin
273	vanXA	CGCTAAATATGCCACTTGGGATA	TCAAAAGCGATTCAGCCAACT	Vancomycin
274	vanXB	AGGCACAAAATCGAAGATGCTT	GGGTATGGCTCATCAATCAACTT	Vancomycin
275	vanXD	TAAACCGTGTTATGGGAACGAA	GCGATAGCCGTCCCATAAGA	Vancomycin
276	vanYB	GGCTAAAGCGGAAGCAGAAA	GATATCCACAGCAAGACCAAGCT	Vancomycin
277	vanYD-01	AAGGCGATACCCTGACTGTCA	ATTGCCGGACGGAAGCA	Vancomycin
278	vanYD-02	CAAACGGAAGAGAGGTCACTTACA	CGGACGGTAATAGGGACTGTTC	Vancomycin

279	vatB-01	GGAAAAAGCAACTCCATCTCTTGA	TCCTGGCATAACAGTAACATTCTGA	MLSB
280	vatB-02	TTGGGAAAAAGCAACTCCATCT	CAATCCACACATCATTTCCAACA	MLSB
281	vatC-01	CGGAAATTGGGAACGATGTT	GCAATAATAGCCCCGTTTCCTA	MLSB
282	vatC-02	CGATGTTTGGATTGGACGAGAT	GCTGCAATAATAGCCCCGTTT	MLSB
283	vatE-01	GGTGCCATTATCGGAGCAAAT	TTGGATTGCCACCGACAAT	MLSB
284	vatE-02	GACCGTCCTACCAGGCGTAA	TTGGATTGCCACCGACAATT	MLSB
285	vgaA-01	CGAGTATTGTGGAAAGCAGCTAGTT	CCCGTACCGTTAGAGCCGATA	MLSB
286	vgaA-02	GACGGGTATTGTGGAAAGCAA	TTTCCTGTACCATTAGATCCGATAATT	MLSB
287	vgb-01	AGGGAGGGTATCCATGCAGAT	ACCAAATGCGCCCGTTT	MLSB
288	vgbB-01	CAGCCGGATTCTGGTCCTT	TACGATCTCCATTCAATTGGGTAAA	MLSB

289	vgbB-02	ATACGAGCTGCCTAATAAAGGATCTT	TGTGAACCACAGGGCATTATCA	MLSB
290	yceE/mdtG-01	TGGCACAAAATATCTGGCAGTT	TTGTGTGGCGATAAGAGCATTAG	Multidrug
291	yceE/mdtG-02	TTATCTGTTTTCTGCTCACCTTCTTTT	GCGTGGTGACAAACAGGCTTA	Multidrug
292	yceL/mdtH-01	TCGGGATGGTGGGCAAT	CGATAACCGAGCCGATGTAGA	Multidrug
293	yceL/mdtH-02	CGCGTGAAACCTTAAGTGCTT	AGACGGCTAAACCCCATATAGCT	Multidrug
294	yceL/mdtH-03	CTGCCGTTAAATGGATGTATGC	ACTCCAGCGGGCGATAGG	Multidrug
295	yidY/mdtL-01	GCAGTTGCATATCGCCTTCTC	CTTCCCGGCAAACAGCAT	Multidrug
296	yidY/mdtL-02	TGCTGATCGGGATTCTGATTG	CAGGCGCGACGAACATAAT	Multidrug

789

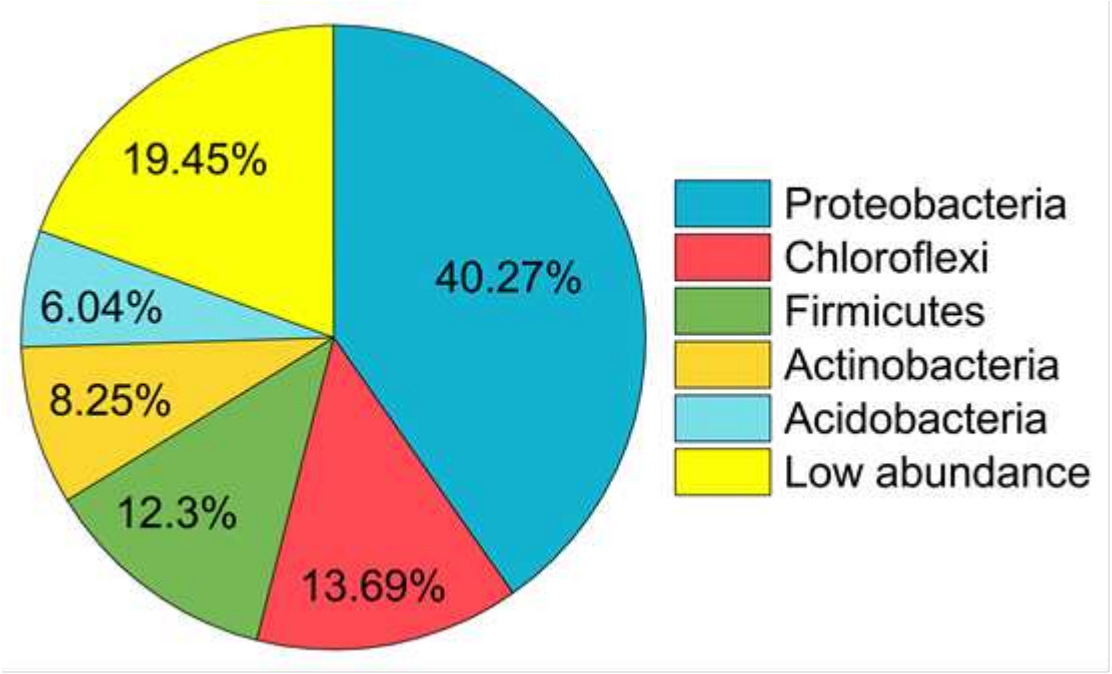

790

791 **Figure S1.** Mean percentage of each bacterial phylum (n = 12) in the nematode
792 microbiome. “Low abundance” consists of phyla with the largest relative abundance <
793 10%.

794

795

796

797

798

799

800

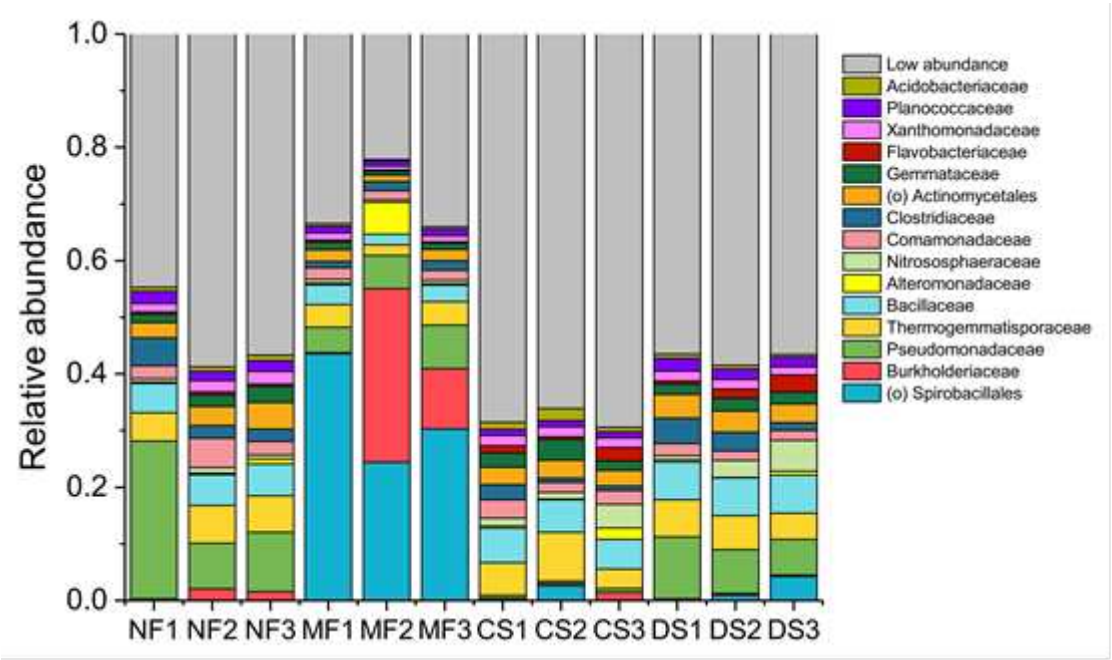

Figure S2. Relative abundance of soil nematode-associated bacteria (family level) in each treatment ("NF", no fertilizer; "MF", mineral fertilizer; "CS", clean slurry; "DS", "dirty slurry"). "Low abundance" consists of the total relative abundance of family < 2%. Unassigned family is indicated using the "Order".

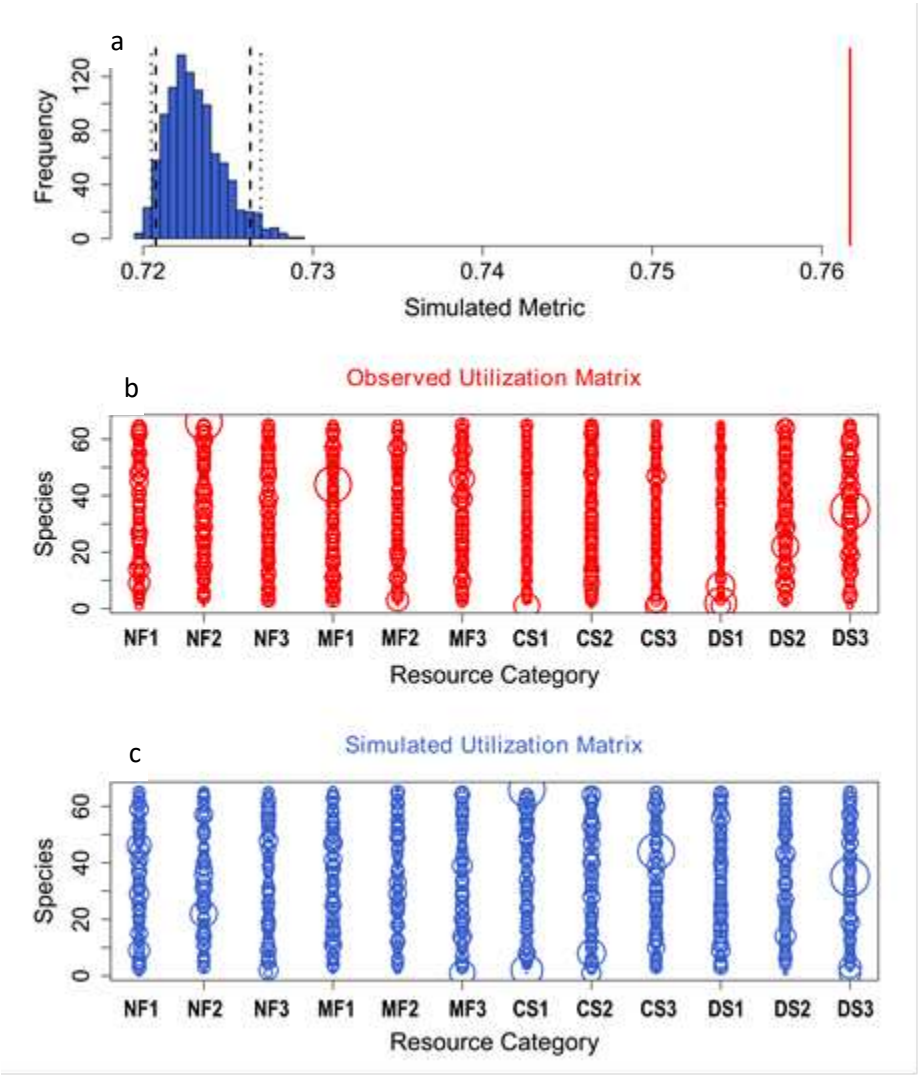

Figure S3. The assembly of soil nematode microbiome. The C-score of soil nematode-associated microbial co-occurrence patterns is indicated by a red line, calculated from the relative abundance of the nematode microbiome at the family level with relative abundance > 0.5%, compared with the score distribution of a simulated metric generated from 5000 random permutations of the same data set (Blue column). The long and short dash lines respectively represent 95% confidence interval for one-tail and two-tail. “NF”, no fertilizer; “MF”, mineral fertilizer; “CS”, clean slurry; “DS”, “dirty slurry”.

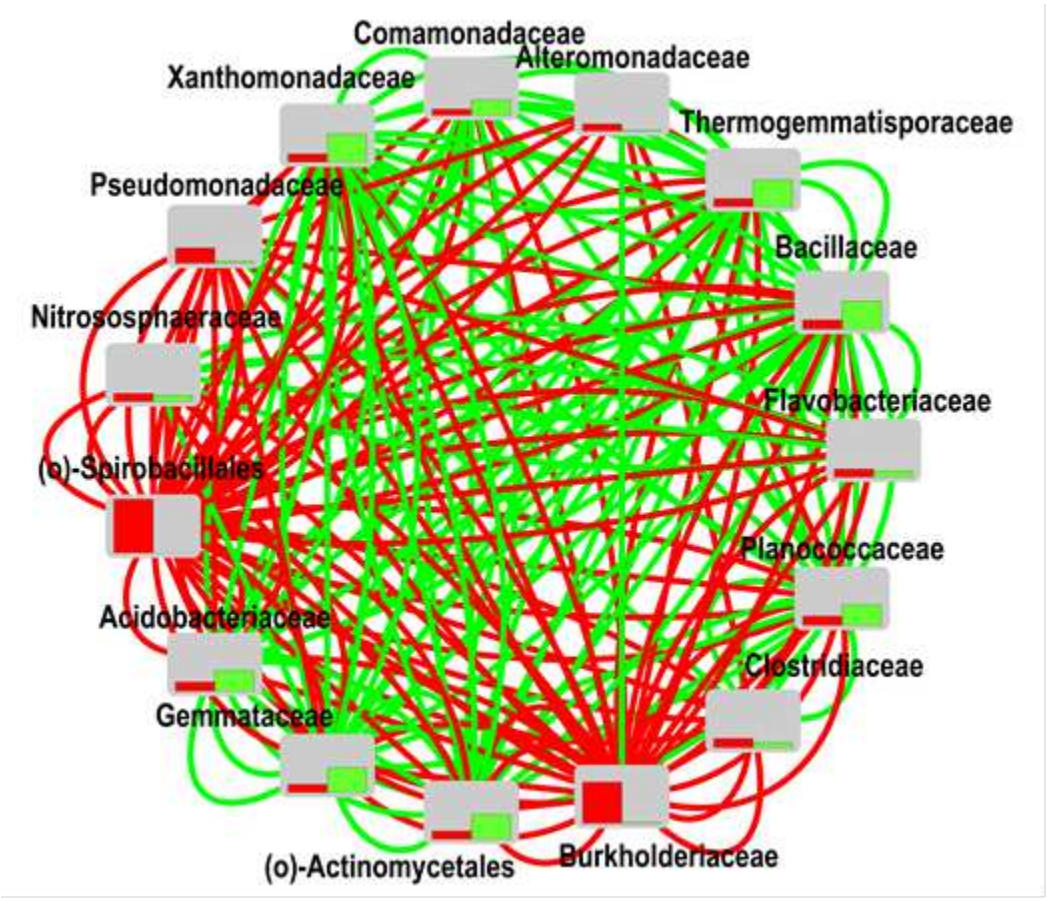

Figure S4. Interaction networks between families with a relative abundance >2% of the nematode microbiome. Green and red lines represent positive and negative interactions, respectively. The balance of interactions (positive versus negative) is indicated by the coloured columns, green (positive) and red (negative).

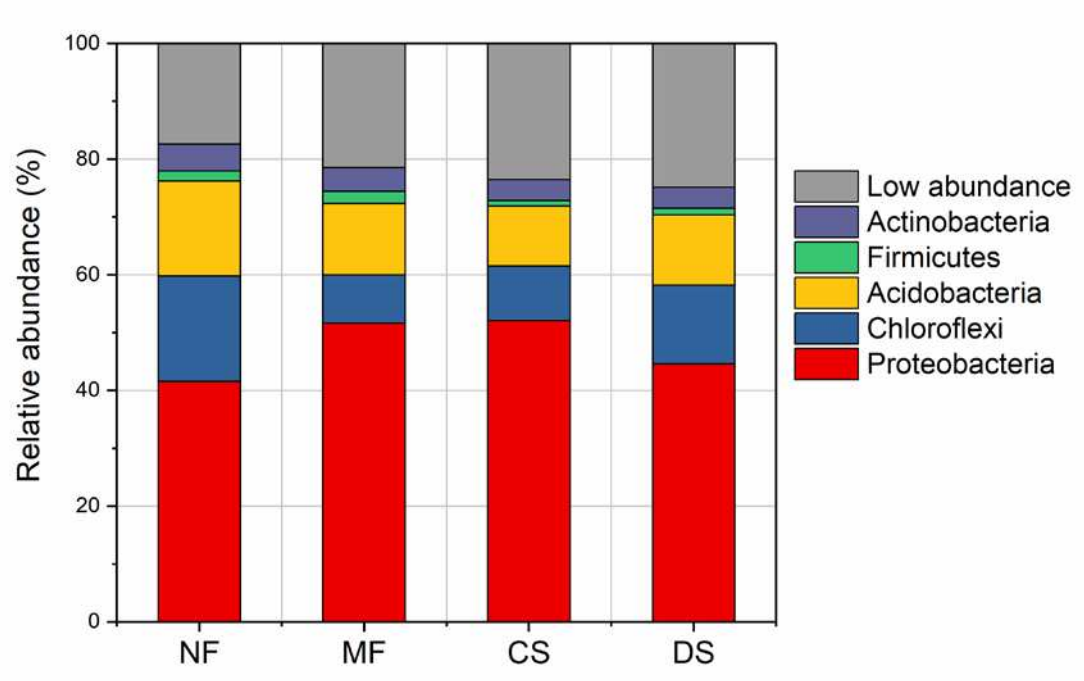

Figure S5. Relative abundance of soil microbiome (phylum level) in each treatment ("NF", no fertilizer; "MF", mineral fertilizer; "CS", clean slurry; "DS", "dirty slurry"). "Low abundance" consists of the total relative abundance of phyla < 5%.

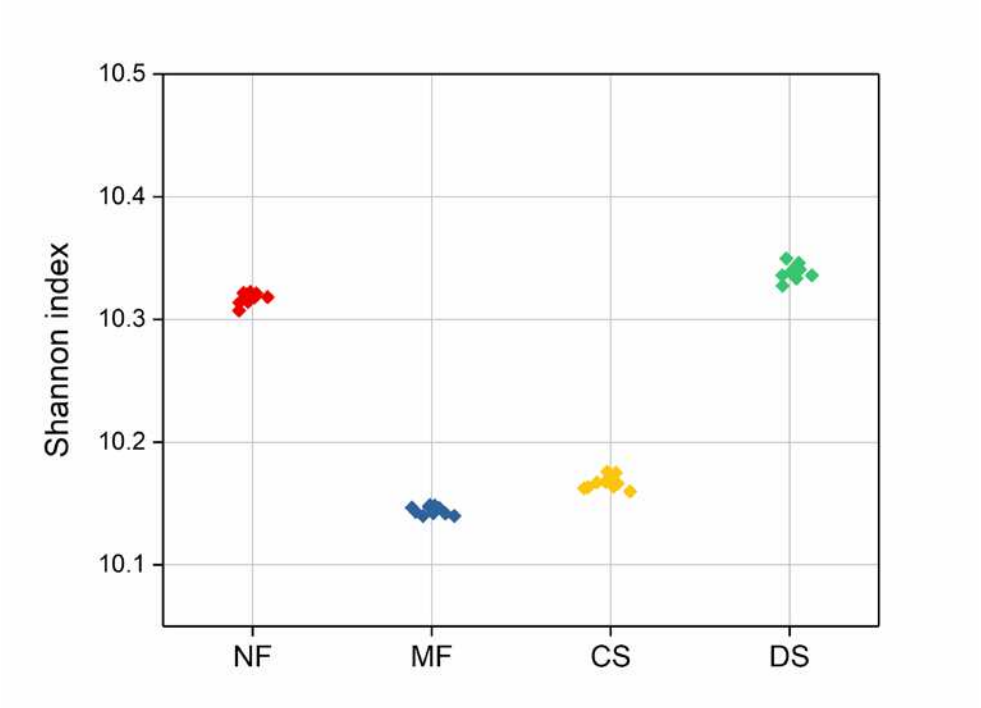

Figure S6. The Shannon index (mean ± SE, n = 3) of the soil microbiome in various treatments indicated by different colours ("NF", no fertilizer; "MF", mineral fertilizer; "CS", clean slurry; "DS", "dirty slurry").

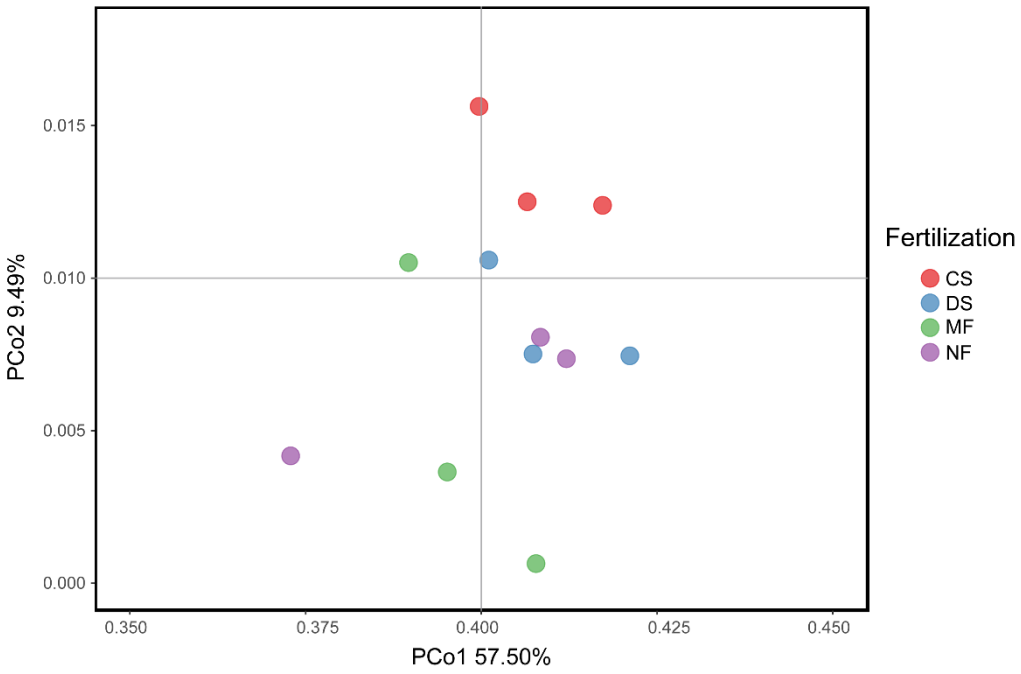

Figure S7. Principal coordinates analysis (PCoA) of the soil microbiome using relative abundance of OTUs based on Bray-Curtis distances. Treatments are indicated by different colours ("NF", no fertilizer; "MF", mineral fertilizer; "CS", clean slurry; "DS", "dirty slurry"). The explained variation is listed in parentheses. The Adonis test was used to compare the difference between treatments (Adonis test, $P > 0.05$).

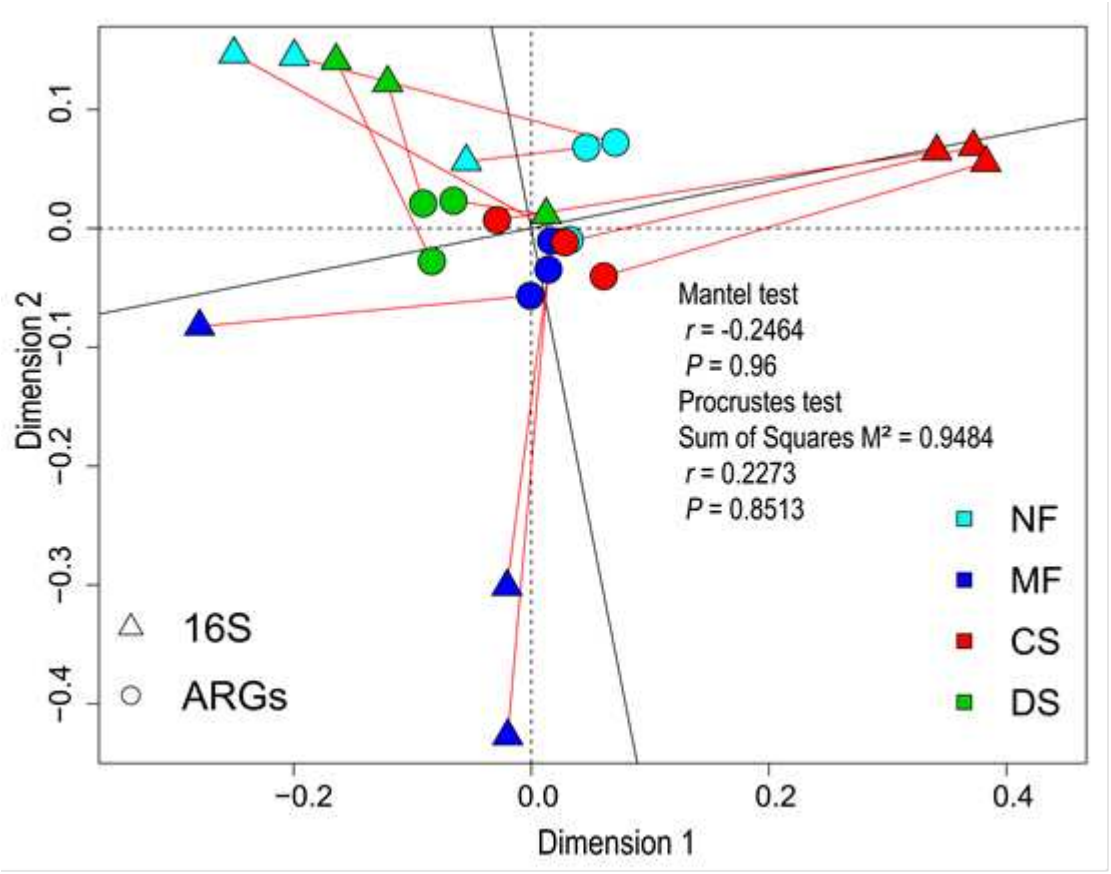

Figure S8. Procrustes test revealing no significant correlation between ARG profiles and nematode microbiome composition (16S rRNA gene OTUs data) based on Bray−Curtis dissimilarity metrics (sum of squares $M^2 = 0.9484$, $P = 0.8513$, 9999 permutations). Triangles represent 16S rRNA gene OTUs nematode microbiome data and the circles indicate ARG profiles. A Mantel test was also conducted to explore the relationship between ARGs and bacterial communities based on Bray-Curtis distance.